 doi:10.20944/preprints202008.0530.v1

Antiviral phytochemicals identified in *Rhododendron arboreum* petals exhibited strong binding to SARS-CoV-2 M^{Pro} and Human ACE2 receptor

Maneesh Lingwan[a#], Shagun Shagun[a#], Yogesh Pant[a], Bandna Kumari[a], Ranjan K Nanda[b], Shyam K Masakapalli[a*]

a) BioX Center, School of Basic Sciences, Indian Institute of Technology Mandi, Kamand 175075, Himachal Pradesh, India

b) Translational Health Group, International Centre for Genetic Engineering and Biotechnology, New Delhi 110067, India

# Joint first author/Equal contribution

* Corresponding author

Shyam K Masakapalli

BioX Center, School of Basic Sciences, Indian Institute of Technology Mandi, Kamand 175075, Himachal Pradesh, India

Tel.: +918628088505

E-mail address: shyam@iitmandi.ac.in

Preprints (www.preprints.org) | NOT PEER-REVIEWED | Posted: 24 August 2020 doi:10.20944/preprints202008.0530.v1

Graphical abstract

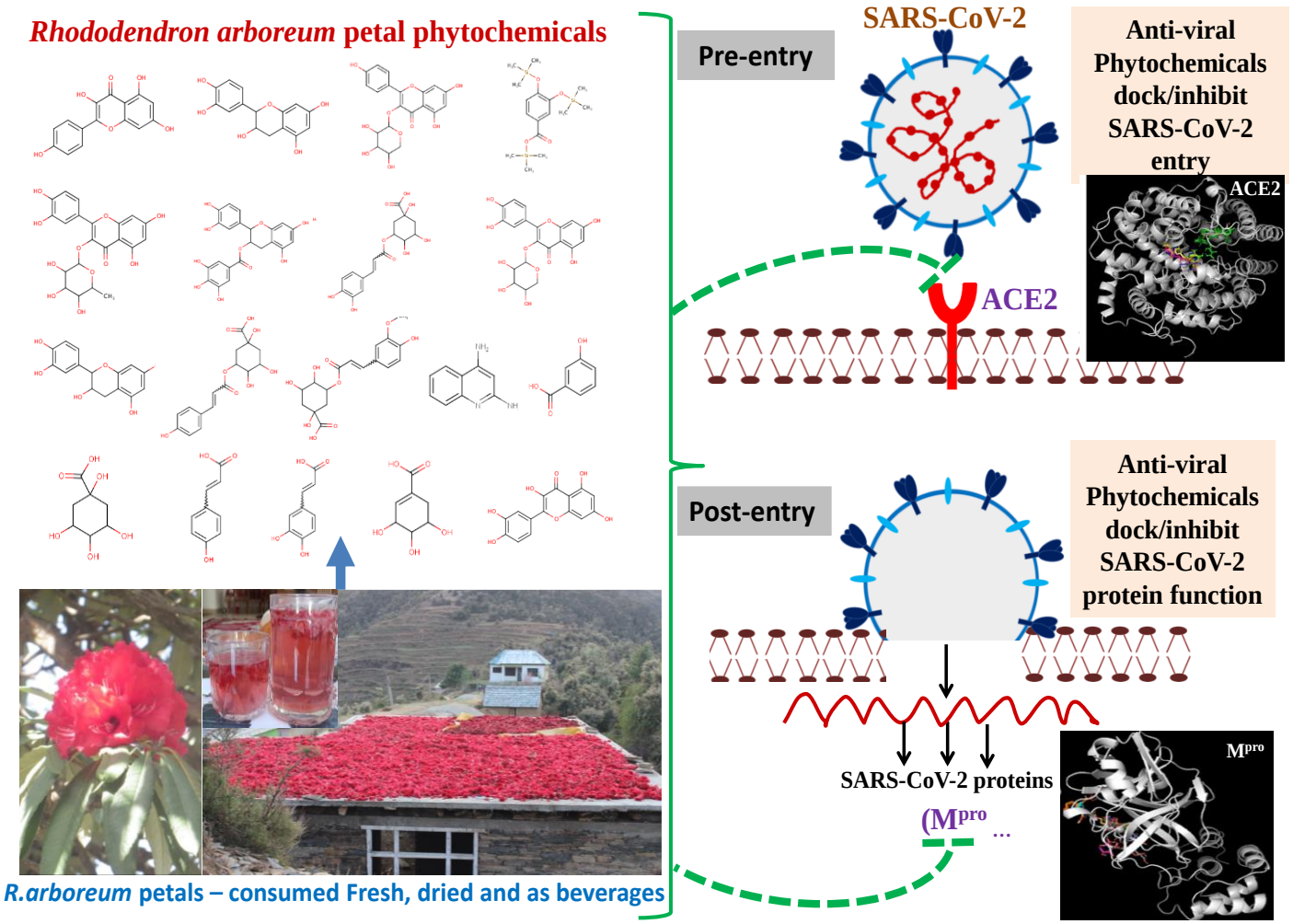

Preprints (www.preprints.org) | NOT PEER-REVIEWED | Posted: 24 August 2020 doi:10.20944/preprints202008.0530.v1

Abstract

Background: Severe Acute Respiratory Syndrome Corona Virus 2 (SARS-CoV-2) affects human respiratory function causing COVID-19 disease. Safe natural products with potential antiviral phytochemicals with benefits to control high-altitude sickness could be adopted as adjunct therapy for COVID-19. The red petals of *Rhododendron arboreum,* commonly available and consumed in the Himalayan region may have phytochemicals with potential antiviral properties against COVID-19 targets.

Purpose: This study was aimed to profile the secondary metabolites of *R. arboreum* petals, to assess their absorption, distribution, metabolism and elimination (ADME) properties and evaluate their antiviral potential by docking against COVID-19 targets such as SARS-CoV-2 main protease (M^{pro} PDB ID: 6LU7) and Human Angiotensin Converting Enzyme 2 (ACE2) receptor (PDB ID: 1R4L) that mediates the viral replication and entry into the host respectively.

Methods: The phytochemicals of *R. arboreum* petals were mainly profiled using Gas Chromatography-Mass Spectroscopy (GC-MS) and ^{1}H-NMR. In addition, the phytochemicals reported from the literature were tabulated. The ADME properties of the phytochemicals were predicted using SwissADME tool. Molecular docking simulation of the phytochemicals against SARS-CoV-2 main protease (M^{pro} PDB ID: 6LU7) and Human Angiotensin converting enzyme 2 (ACE2) receptor (PDB ID: 1R4L) were carried out using PyRx.

Results: *R. arboreum* petals were found to be rich in appreciable proportions of secondary metabolites such as Quinic acid, 3-Caffeoyl-quinic acid, 5-O-Coumaroyl-D-quinic acid, 5-O-Feruloylquinic acid, 2,4-Quinolinediamine, Coumaric acid, Caffeic acid, Epicatechin, Catechin, 3-Hydroxybenzoic acid, Shikimic acid, Protocatechuic acid, Epicatechin gallate, Quercetin, Quercetin-O-pentoside, Quercetin-O-rhamnoside, Kaempferol-O-pentoside and Kaempferol. Several of these phytochemicals were reported to exhibit inhibitory activities against a range of viruses. From the molecular docking studies, 5-O-Feruloylquinic acid, 3-Caffeoyl-quinic acid, 5-O-Coumaroyl-D-quinic acid, Epicatechin and Catechin showed strong binding affinity with SARS-CoV-2 M^{pro} and human ACE2 receptor.

Conclusion: This report showed that R. *arboreum* petals are rich in several antiviral phytochemicals that also docked against SARS-CoV-2 M^{Pro} and Human ACE2 receptor. This is the first report highlighting *R. arboreum* petals as a reservoir of antiviral phytochemicals with potential for synergetic activities. The outcomes merit further *in vitro, in vivo* and clinical studies on *R. arboreum* phytochemicals to develop natural formulations against COVID-19 disease for therapeutic benefits.

Keywords: *R. arboreum*, Antiviral phytochemicals, SARS-CoV-2, M^{Pro}, ACE2, COVID-19

 doi:10.20944/preprints202008.0530.v1

Abbreviations

SARS-CoV-2, Severe Acute Respiratory Syndrome Corona Virus 2; ADME, absorption, distribution, metabolism and elimination; ACE2, Angiotensin Converting Enzyme 2; GC-MS, Gas Chromatography-Mass Spectroscopy; NMR, Nuclear Magnetic Resonance; MSTFA, N-Methyl-N-(trimethylsilyl) trifluoroacetamide; TIC, Total ion chromatograms; DSS, 4,4-dimethyl-4-silapentane-1-sulfonic acid; PDB, Protein Data Bank; CASTp, Computed Atlas for Surface Topography of Proteins; DPPH, 2,2-diphenyl-1-picrylhydrazyl; HAPE, High altitude pulmonary edema; CQA, Caffeoylquinic acid.

1. Introduction

Rhododendron is an important genus found abundantly in the Himalayas with reported application of its various plant parts for medicinal and commercial uses (Kumar et al., 2019). In the western mid-Himalayas, *Rhododendron arboreum* is one of the abundant species with distinct red coloured flowers which are traditionally used in culinary, as juice, squash and wine preparation. Flowers of *R. arboreum* is reported to be rich source of many bioactive compounds with antimicrobial, antioxidant (Srivastava, 2012), anti-inflammatory and cholinergic activity (Agarwal & Kalpana, 1988). In addition, the anthocyanidins present in the flower petals are also reported to possess antioxidant (Tsuda et al., 1994), antidiabetic (Tsuda et al., 2003), anticarcinogenic (Hagiwara et al., 2001) activities and useful in treating inflammation and damage caused by UV in liposomes (Min et al., 2010). Flower juice is used in the treatment of menstrual disorders (Uniyal et al., 2006). The dried flowers are very useful in controlling diarrhoea and dysentery (Laloo et al., 2006). Here, in the mid-Himalayan region of Himachal Pradesh where our laboratory is based, we observed that the local villagers use the *R. arboreum* petals for making chutney and beverages (as squash, juice, wine) providing them with a sustainable source of income. Although widely used, the phytochemical or metabolite profiles of the petals need chemical characterization.

The Gas Chromatography-Mass Spectroscopy (GC-MS) and ^{1}H Nuclear Magnetic Resonance (NMR) Spectroscopy based analysis of the petal extracts will be useful to identify and validate the presence of antiviral phytochemicals. Coronavirus disease (COVID-19) is caused by Severe Acute Respiratory Syndrome Corona Virus 2 (SARS-CoV-2), which spread worldwide and caused a pandemic. Coronaviruses are the enveloped viruses having positive-sense, single-strand RNA (Huang et al., 2020). Coronaviruses (CoVs) infects several species of animals including mammals, birds and reptiles and can cause severe respiratory diseases. Since the beginning of 21st century, these viruses have caused major outbreaks leading to human fatal pneumonia and pandemics (Cheng et al., 2007; Malik et al., 2020). Given its uncontrolled ability to infect, there is a need to develop vaccines and drugs

Preprints (www.preprints.org) | NOT PEER-REVIEWED | Posted: 24 August 2020 doi:10.20944/preprints202008.0530.v1

which also includes deploying plant-based phytochemicals for its control. SARS-CoV-2 virus enters and replicate within the host cells mediated by its different structural and functional proteins. Spike protein of the SARS-CoV-2 binds to Angiotensin-converting enzyme 2 (ACE2), a receptor that mediates the entry of the virus into the human host cell (Wan et al., 2020). Small molecules that can inhibit the catalytic site of the ACE2 protein may provide a suitable therapeutic strategy to block the entry of coronavirus into the host cells. Once, inside the host cell; the main protease (M^{pro}) of SARS-CoV-2 play vital role in the polyprotein processing and virus maturation (Liu and Wang, 2020). Two replicase polyproteins are cleaved by the main protease of the virus which is required to mediate viral replication and transcription. Inhibition of the protease activity might also significantly affect the viral replication (Zhang et al., 2020). Therefore, M^{pro} provides another important target for the discovery and development of an antiviral drug.

The current study is focused on profiling the secondary metabolites present in *R. arboreum* petals, assess their absorption, distribution, metabolism and elimination (ADME) properties and investigate their binding affinity with SARS-CoV-2 main protease (M^{pro}) and ACE-2 host cell receptor protein using molecular/computational docking studies. It has been observed that *R. arboreum* petals are enriched with antiviral phytochemicals with promising ability to strongly bind with the COVID-19 targets. The outcomes further warrant *in vivo*, *in vitro* and clinical testing of *R. arboreum* petals against COVID-19 to formulate safe and natural antiviral phytochemical extracts.

2. Material and methods

2.1. Harvesting and processing of Plant materials

The magnificent red flowers of *Rhododendron arboreum* were collected from the mid-Himalayan region in Mandi district in the hills between IIT Mandi and Parashar lake area (>2000m Height above mean sea level (AMSL), Himachal Pradesh, India. The petals were separated, washed with water and air dried under shade. The dried petals were powdered and stored at -20 ^{o}C for subsequent analysis at the medicinal plant laboratory of IIT Mandi.

2.2. Estimation of total phenols and antioxidant capacities of *Rhododendron* petal extracts

The powder of *R. arboreum* petals (100 mg dry weight: DW powder) was mixed in acetone (70 %, 2 ml). The extract was vortexed and centrifuged at 10,000 rpm for 10 min at 4 °C. The supernatant was used for total phenol content estimation using Folin-Ciocalteu method (Kupina et al., 2019). Acetone extract (100 µl) was mixed with Folin-Ciocalteu reagent (10 % v/v in MiliQ water, 500 µl) and incubated for 5 min at room temperature. The reaction was initiated by adding 400 µl sodium carbonate (5 % w/v in water) and incubated for 20 min at room temperature. Total soluble phenols

were analysed at absorbance 765 nm, calibrated against gallic acid as standard (0.02 mg/ml to 0.1 mg/ml). For determination of 2,2-diphenyl-1-picrylhydrazyl (DPPH) radical-scavenging activity, phytochemical extract from dry petal powder (5 mg in 1 ml water) was used. Briefly, the extract was centrifuged at 10,000 × g for 15 min at 4 °C and supernatant was collected. DPPH solution (0.1 mM, prepared in absolute ethanol, 900 µl) was mixed with varying concentration of sample extract (100 µl; 0.25, 0.5, 1, 2, 4, 5 mg/ml), vortexed and incubated in room temperature for 30 min under dark. The antioxidant activity was calculated by measuring the absorbance at 517 nm after completion of the incubation period (Maiti et al., 2014). From the absorbance IC50 (50% inhibitory concentration) values were calculated and compared with positive control (ascorbic acid, 0.01-0.1 mg/ml).

2.3. Extraction of *R. arboreum* petal phytochemicals

Water extract of *R. arboreum* petals (50 mg DW in 1 ml water) was prepared by heating at 70 °C for 5 min in a dry bath with continuous shaking at 500 rpm. Prior to the extraction, Ribitol (0.01 mg ml^{-1}) was added as an internal standard. This extract is centrifuged at 10,000 × g for 15 min at room temperature. The supernatant containing hot water-soluble metabolites were transferred to a new fresh eppendorf tube. Aliquots of 50 µl and 20 µl were dried under-speed vacuum evaporator for phytochemical profiling using Gas Chromatography-Mass Spectrometry (GC-MS) (Lisec et al., 2006; Shree et al., 2019) and ^{1}H NMR analysis.

2.4. Phytochemical profiling *R. arboreum* petals using Gas Chromatography-Mass Spectrometry

The dried aliquots of hot water-soluble extracts of *R. arboreum* petals were derivatised by adding pyridine (50 µl) containing methoxyamine hydrochloride (20 mg/ml) followed by incubation at 37 °C at 900 rpm for 2 hours and then MSTFA (N-Methyl-N- (trimethylsilyl) trifluoroacetamide, 70 µl) was added and incubated at 37 °C, 900 rpm for 30 min. The derivatised samples were centrifuged at 13,000 g for 10 min. The clear supernatant (100 µl) was transferred to a fresh vial and subjected to GC-MS data acquisition (Agilent instrument). The molecules were separated using a DB-5ms column (30 m x 250 µm x 1 µm). Helium was used as carrier gas at a flow rate of 0.6 ml/min. The front inlet temperature was 250 °C. The GC temperature program used was from 60 °C to a final 200 °C oven temperature gradient with an increase of 10 °C/min and hold time for 4 min. Further, ramped to a final 300 °C temperature at 10 °C/min and a hold time of 10 min at highest temperature. The total run time was 60 min. The raw GC-MS data were pre-processed for baseline correction. The metabolic features in total ion chromatograms (TIC) were further annotated against available commercial standards and match score of minimum 70 % against the libraries NIST17 (National Institute of Standards and

Preprints (www.preprints.org) | NOT PEER-REVIEWED | Posted: 24 August 2020 doi:10.20944/preprints202008.0530.v1

Technology, Maryland) and Fiehn13 (Agilent Technologies, USA). Retention times (RT), m/z fragmentation patterns and peak areas were extracted (Masakapalli et al., 2014a, Yadav et al., 2019).

2.5. ^{1}H NMR spectroscopy analysis of *R. arboreum* petal extracts

Aliquots (500 µl) of hot aqueous extracts were vacuum dried in an eppendorf tube and was reconstituted in of deuterated water (D_2O, 650 µl) containing internal standard 4,4-dimethyl-4-silapentane-1-sulfonic acid (DSS, 0.01 % w/v). The reconstituted sample was vortexed for 5 min and transferred into a 5 mm NMR tube. The ^{1}H NMR spectra were recorded on JEOL–ECX 500 NMR instrument for 64 scans, with a relaxation delay of 5s. The spectra obtained were manually corrected for phase and baseline distortions and referenced to DSS (set at 0 ppm) using software package JEOL Delta. ^{1}H-NMR spectra of the quinic acid standard were also recorded to confirm its identity in test samples (Masakapalli et al., 2014b).

2.6. Prediction of physicochemical, ADME pharmacokinetics, drug-likeness and medicinal chemistry properties of *R. arboreum* petal phytochemicals

The absorption, distribution, metabolism, elimination (ADME) properties of the extracted and reported phytochemicals of *R. arboreum* petals were probed using SwissADME (Daina et al., 2017). The physicochemical properties, lipophilicity, water-solubility, pharmacokinetics, drug-likeness and medicinal chemistry of the phytochemicals were evaluated using various parameters (Cheng et al., 2012; Pires et al., 2015). For the computational simulation, canonical SMILES of the selected phytochemicals were obtained from PubChem database (Bolton et al., 2008) and incorporated into SwissADME tool for the prediction of the properties.

2.7. Molecular docking simulation of *R. arboreum* petal phytochemicals

2.7.1. COVID-19 target proteins selected for docking

The three dimensional crystal structures of the target proteins: SARS-CoV-2 main protease (PDB ID: 6LU7) (Jin et al., 2020) and Angiotensin Converting Enzyme 2 (ACE2) receptor of host cell (PDB ID: 1R4L) (Towler et al., 2004) were retrieved from Protein Data Bank (Bernstein et al., 1978). Removal of water molecules, metal ions and all the native ligands bound to the target protein molecules was carried out by using Biovia Discovery studio client 2020 (https://discover.3ds.com/discovery-studio-visualizer-download).

2.7.2. Phytochemical ligands from *R. arboreum* petals

Preprints (www.preprints.org) | NOT PEER-REVIEWED | Posted: 24 August 2020 doi:10.20944/preprints202008.0530.v1

The three-dimensional structures of the *R. arboreum* petal phytochemicals were obtained from PubChem in SDF (Spatial Data file) format (Kim et al., 2019). The small molecules used for the docking studies against target proteins were 2,4-Quinolinediamine (CID: 14207924), 3-Hydroxybenzoic acid (CID: 7420), 4-Coumaric acid (CID: 637542), 5-O-Feruloylquinic acid (CID: 9799386), Caffeic acid (CID: 689043), Catechin (CID: 9064), 3-Caffeoyl-quinic acid (CID: 1794427), Epicatechin (CID: 72276), Protocatechuic acid (CID: 72), Shikimic acid (CID: 8742), 5-O-Coumaroyl-D-quinic acid (CID: 6441280), Quinic acid (CID: 6508), Quercetin (CID: 5280343), Quercetin-O-pentoside (CID: 5878729), Kaempferol-O-pentoside (CID: 14749097), Kaempferol (CID: 5280863), Epicatechin gallate (CID: 107905) and Quercetin-O-rhamnoside (CID: 5280459). Glycyrrhizic acid (CID: 14982) was reported to dock against SARS-CoV-2 main protease (PDB ID: 6LU7) and Angiotensin converting enzyme 2 (ACE2) receptor of host cell (PDB ID: 1R4L) and hence is selected as positive control for comparative analysis (Zhang et al., 2020).

2.7.3. Determination of Active Sites of target proteins

The amino acids present in the active site pocket of the target proteins were determined by Computed Atlas for Surface Topography of Proteins (CASTp) (Tian et al., 2018). These amino acids present in the active sites pockets of the target proteins were used for the creation of the grid box and analysis of the docking results.

2.7.4. Molecular Docking of *R. arboreum* petal phytochemicals

PyRx Virtual Screening software (version 0.8) was used for the docking simulations (Dallakyan and Olson, 2015). Prior to docking, the target protein molecules and ligands were converted to the PDBQT files. Firstly, we performed the blind docking to analyse the binding of ligands with the proteins. After the blind docking, active site docking was performed. Docking of the selected ligands against the target proteins was carried out using AutoDock Vina assembled in the PyRx software. Higher the negative binding affinity value, the stronger is the binding of the ligand to the target, so the conformation with the lowest binding affinity was chosen. Analyses of the docking results were carried out by using the software Biovia Discovery studio client 2020 and PyMOL2.4 (http://www. pymol. org). The binding affinities of the *R. arboreum* phytochemicals were compared with the positive control i.e. Glycyrrhizic acid.

3. Results

3.1. *Rhododendron* petal extracts constitute polyphenols and exhibit antioxidant ability

Preprints (www.preprints.org) | NOT PEER-REVIEWED | Posted: 24 August 2020 doi:10.20944/preprints202008.0530.v1

The total polyphenol and DPPH radical scavenging activity of *R. arboreum* petal extracts were measured. Total polyphenols were measured to be 59.87 mg GAE (gallic acid equivalent)/g of petal. The DPPH radical scavenging activity showed that *R. arboreum* petal extracts possess antioxidant ability with IC_{50} of 0.98 ± 0.01 mg/ml of petal extract which is comparable to the IC_{50} of ascorbic acid in concentration range of 0.01-0.1 mg ascorbic acid/ml.

3.2. *R. arboreum* petals are rich in secondary metabolites

The GC-MS profiles of hot aqueous extracts from *R. arboreum* petals confirmed appreciable proportion of secondary metabolites covering ~32 % peak area in comparison to other phytochemicals such as sugars, organic acids and amino acids **(Fig. 1A).** The secondary metabolites detected were Quinic acid, 3-Caffeoyl-quinic acid, 5-O-Coumaroyl-D-quinic acid, 5-O-Feruloylquinic acid, 2,4-Quinolinediamine, Coumaric acid, Caffeic acid, Epicatechin, Catechin, 3-Hydroxybenzoic acid, Shikimic acid and Protocatechuic acid **(Table S1).** Also, ^{1}H-NMR of *R. arboreum* petals confirmed appreciable proportion of quinic acid and its derivatives **(Fig. 1B).** We also selected molecules reported from earlier work of Shresta 2016 on *R. arboreum* petals like Epicatechin gallate, Quercetin, Quercetin-O-pentoside, Quercetin-O-rhamnoside, Kaempferol-O-pentoside and Kaempferol for further analysis **(Table S1).**

3.3. Physicochemical, ADME, pharmacokinetics, drug-likeness and medicinal chemistry properties of *R. arboreum* petal phytochemicals

The prediction of physicochemical, ADME, pharmacokinetics, drug-likeness and medicinal chemistry friendliness properties of phytochemicals, present in *R. arboreum* petal, by SwissADME tool (Daina et al., 2017). Most of the molecules exhibited promising ADME properties with few exceptions (**Table S2**). This is supported by the prediction of a range of parameters such as the phytochemical structures, Topological Polar Surface Area, The LogP values, Log S, bioavailability, log Kp values and Lipinski's rules (**Table S2**).

3.4. Molecular docking of *R. arboreum* phytochemicals predicted their potential antiviral properties against the COVID-19 target proteins

The Molecular docking study showed that all the molecules (n=18) were binding with both the target proteins with varying binding parameters (Table S4). For the active site docking, the amino acid residues present in the active site pocket of the target proteins were determined and enlisted. Table S3 present the target protein structures in complex with the native ligand highlighting amino acids found in the active sites of the target proteins. All the phytochemicals screened showed significant binding

Preprints (www.preprints.org) | NOT PEER-REVIEWED | Posted: 24 August 2020 doi:10.20944/preprints202008.0530.v1

affinity to the SARS-CoV-2 main protease and human host cell receptor ACE2 protein. Out of all the molecules docked, 5-O-Feruloylquinic acid, 3-Caffeoyl-quinic acid, 5-O-Coumaroyl-D-quinic acid, Epicatechin and Catechin showed strong binding affinity with the two target proteins.

3.4.1. The phytochemicals of *R. arboreum* petals docked well to SARS-CoV-2 main protease (SARS-CoV-2 M^{pro})

Active site docking of all the 18 petal phytochemicals against the SARS-CoV-2 main protease M^{pro} (6LU7) which is essential for viral replication was performed. The docking results including the binding affinities, active site amino acid residues and various types of interactions between the phytochemicals and SARS-CoV-2 main protease **(Fig. 2, Fig. S1, Fig. S2, Fig. S3, Fig. S4 and Table 1).** Several of the phytochemicals screened showed significant binding ability towards M^{pro} and showed interactions with the active site amino acids. Binding affinities of the molecular docking studies - Epicatechin gallate (-7.3 kcal/mol), 5-O-Feruloylquinic acid (-7.2 kcal/mol), 5-O-Coumaroyl-D-quinic acid (-7.2 kcal/mol), Quercetin-O-rhamnoside (-7.2 kcal/mol), 3-Caffeoyl-quinic acid (-7.1 kcal/mol), Quercetin-O-pentoside (-7.1 kcal/mol), Kaempferol (-7.1 kcal/mol), Epicatechin (-7 kcal/mol), Catechin (-6.7 kcal/mol), Quercetin (-7 kcal/mol), and Kaempferol-O-pentoside (-7 kcal/mol) (Table 1). These molecules showed very strong interactions with the SARS-CoV-2 M^{pro} active sites amino acid residues THRA:24, THRA:25, THRA:26, GLYA:143, LEUA:27, THRA:45, SERA:46, CYSA:145, HISA:164, ASPA:187, HISA:41, ARGA:188, META:49, GLNA:189, GLUA:166, THRA:190, ALAA:191 etc **(Fig. 2, Fig. S4 and Table 1).**

3.4.2. The phytochemicals of *R. arboreum* petals docked well to Human Angiotensin Converting Enzyme 2 (ACE2) receptor

Active site docking of all the 18 petal phytochemicals against the human ACE2 receptor protein (PDB ID: 1R4L) was performed. Molecular docking studies showed strong binding affinities, involved active site amino acid residues and various types of interactions between the phytochemicals and human cell receptor ACE2 **(Fig. 3, Fig. S5, Fig. S6, Fig. S7, Fig. S8 and Table 2).** Several of the phytochemicals screened showed significant binding ability towards ACE2 and showed interactions with the active site amino acids. The following binding affinities are observed from docking studies Quercetin-O-rhamnoside (-10.2 kcal/mol), Epicatechin gallate (-10.1 kcal/mol), Quercetin-O-pentoside (-9.9 kcal/mol), Kaempferol-O-pentoside (-9.7 kcal/mol), Catechin (-9 kcal/mol), Quercetin (-8.9 kcal/mol), 5-O-Feruloylquinic acid (-8.6 kcal/mol), 3-Caffeoyl-quinic acid (-8.5 kcal/mol), 5-O-Coumaroyl-D-quinic (-8.5 kcal/mol), Kaempferol (-8.4 kcal/mol) and Epicatechin (-8.4 kcal/mol) (Table 2). These molecules showed very strong interactions with the ACE2 active sites amino acid residues such as

PHEA:32, GLUA:37, PHEA:40, SERA:43, SERA:44, SERA:47, TYRA:50, ASNA:52, ILEA:54, META:62, ASNA:63, GLYA:66, ASPA:67, TRPA:69, SERA:70, ALAA:71, LEUA:73, LYSA:74, SERA:77, LEUA:91, THRA:92, LYSA:94, LEUA:95, GLNA:96, GLNA:98, ALAA:99, LEUA:100, GLNA:102, ASNA:103, GLYA:104, SERA:105, SERA:106, LEUA:108, GLUA:110, SERA:113, LYSA:114, LEUA:116, ASNA:117, LEUA:120, ASNA:121, SERA:124, TYRA:127, SERA:128, THRA:129, GLYA:130, LYSA:131, CYSA:141, LEUA:142, LEUA:143, LEUA:144, GLUA:145, PROA:146, ASNA:149, GLUA:150 etc **(Fig. 3, Fig. S8 and Table 2).**

4. Discussion

COVID-19 caused by SARS-CoV-2 affects human respiratory function, compromises the pO2 level in severe cases with patterns similar to that of high altitude pulmonary edema (HAPE) (Solaimanzadeh, 2020). Recently, dexamethasone, a high-altitude prophylaxis drug for the prevention of acute mountain sickness (Zell and Goodman, 1988) has shown promise in treating a proportion of severe COVID-19 cases (Horby et al., 2020). These observations support our hypothesis that any safe natural product used traditionally to control high-altitude sickness along with potential antiviral phytochemicals may act as the first line of defence against COVID-19.

In the Himalaya's, the flowers of *Rhododendron arboreum* is being traditionally consumed by local population as beverage, squash, chutneys, jams and jellies and believed to help in preventing high-altitude sickness (Devi et al., 2018). The red petals and its extracts exhibit anti-diabetic, anti-diarrhoea, anti-microbial, anti-inflammatory, hepato-protective and anti-oxidant activities (Kumar et al., 2019). *R. arboreum* flower aqueous extract showed significant anti-inflammatory and anti-nociceptive properties against all phlogistic agents (Agarwal and Kalpana, 1988; Verma et al., 2011). Acetate fraction of *R.arboreum* flower extract was reported to be effective against hepatic damage (Verma et al., 2011). The flower extracts given orally showed efficient cholesterol reduction, and enhanced anti-diabetic activity (Bhandary and Kawabata, 2009; Thangaraj, 2013). The antimicrobial activity of the aqueous and ethanolic extract was proven earlier against *E. coli* and *S. aureus* (Sonar et al., 2012). The primary aim of this study was to profile the secondary metabolites present in *R. arboreum* petals, assessing their ADME and their antiviral properties using molecular docking.

Our analysis showed that *R. arboreum* petal extracts constituted higher polyphenol levels in comparison to that of *Rhododendron ponticum* (Malkoc et al., 2016). Also, the capability of the *R. arboreum* petal extracts to scavenge DPPH free radicals are due to the presence of polyphenols with antioxidant properties. Polyphenols are known to have health beneficial effect on humans and act as cardio-protectant, protect cell constituents against oxidative damage, anti-cancerous, neuroprotective

and anti-ageing (Harman, 2006) thereby rendering the significance of *R. arboreum* flower extracts for health.

We profiled the hot aqueous extracts of *R. arboreum* petals using GC-MS which confirmed appreciable proportion of secondary metabolites covering ~32 % peak area in comparison to other phytochemicals such as sugars, organic acids and amino acids **(Fig. 1A).** Predominantly, we observed that the extracts are enriched with secondary metabolites that have potential as antiviral natural products **(Table S5)** as discussed below.

Quinic acid is reported as a potent antiviral molecule with activities against various targets of dengue virus and hepatitis B virus (Li et al., 2005; Mahmood et al., 1993; Wang et al., 2009; Zanello et al., 2015). Molecular simulations/docking study showed the effective binding of quinic acid to the reverse transcriptase enzyme thus possess anti-HIV-1-RT activity (Yazdi et al., 2019). Caffeoylquinic acid (CQA) is one of the potent polyphenols also reported to exhibit activities against hepatitis B virus, influenza viruses (H1N1, H3N2, H5N1), enterovirus 71, herpes virus and HIV (Ding et al., 2017; Li et al., 2013; Ren et al., 2019; Serina et al., 2017; Urushisaki et al., 2011; Wang et al., 2009). The docking simulations/molecular docking between caffeoylquinic acid and the Avian influenza H5N1 neuraminidase showed positive interaction (Ren et al., 2019). Catechins are reported activities against influenza (Song et al., 2005), hepatitis B virus (Li et al., 2001) and docking against ACE2 receptor (Jena et al., 2019). Epicatechin has been reported against Mayaro virus (Ferreira et al., 2018). The antiviral activities of phytochemicals from *R. arboreum* petal extracts such as Caffeic acid, Kaempferol, Quercetin, Shikimic acid, 4-Coumaric acid and other are tabulated **(Table S5).** These reports suggest that *R. arboreum* petal extracts which are rich in various derivatives of Quinic acid (CQA, Feruloyl quinic acid, Coumaroyl quinic acid etc.) could be promising antiviral products.

The potential of the *R. arboreum* petal phytochemicals against COVID-19 targets were further evaluated using molecular docking. This approach has shown promising potential in identifying potential inhibitors against SARS-CoV-2 targets (Pandit and Latha, 2020, Khaerunnisa et al. 2020, Adem et al., 2020). In this study, the molecular docking simulations of the *R. arboreum* petal phytochemicals against the SARS-CoV-2 main protease (M^{pro}) and human cell receptor protein ACE2 which are essential for the viral entry was investigated. The docking analysis showed that most of the *Rhododendron* phytochemicals bind effectively to both the target proteins. It was observed that the molecules exhibited strong binding affinity to human ACE2 protein as compared to the SARS-CoV-2 main protease **(Table 1 and Table 2).** Some of the phytochemicals possess similar binding affinity with the target proteins as glycyrrhizic acid which was used a control. Among all the phytochemicals docked, 5-O-Feruloylquinic acid, 3-Caffeoyl-quinic acid, 5-O-Coumaroyl-D-quinic acid, Epicatechin and Catechin showed the strong binding affinity with ACE2 and SARS-CoV-2 M^{Pro}. The docking

analysis further supports the hypothesis that several of these *R. arboreum* petal phytochemicals might synergistically act as antivirals inhibiting the binding sites of the SARS-CoV-2 and hence merits further *in vivo, in vitro* studies.

The physicochemical, ADME, pharmacokinetics, drug-likeness and medicinal chemistry properties of most of the *R. arboreum* petal phytochemicals showed promising features. It must be noted that the extracts are already used widely by the local population in the Himalayas and hence are largely considered to be safe for human consumption. However, further studies directed towards dosage and scientific assessment against SARS-CoV-2 will provide much needed insights and more importantly the molecular pathways.

Conclusion

In this study, the secondary metabolite of *R. arboreum* petals were deciphered, and their antiviral properties against selected COVID-19 targets using molecular docking were investigated. Several of the secondary metabolites of *R. arboreum* petals docked well against SARS-CoV-2 main protease (M^{pro} PDB ID: 6LU7) and Angiotensin converting enzyme 2 (ACE2) receptor (PDB ID: 1R4L) of humans. Among all the phytochemicals docked, 5-O-Feruloylquinic acid, 3-Caffeoyl-quinic acid, 5-O-Coumaroyl-D-quinic acid, Epicatechin and Catechin showed the strong binding affinity with ACE2 and SARS-CoV-2 M^{pro}. Our results indicate that the hot water extract of *R. arboreum* is rich in antiviral phytochemicals that merits further *in vitro*, *in vivo* and clinical studies to examine its efficacy and develop natural formulations against COVID-19 as adjunct therapeutics.

Acknowledgements

SKM acknowledges Seed Grant of IIT Mandi (IITM/SG/SKM/48) and MHRD-SPARC grant (Project ref P830). RKN acknowledges ICGEB core support. ML, SS, YP acknowledge MHRD, IIT Mandi and SERB for Ph.D. fellowship. Dr Manu Shree is acknowledged for assisting in running the GC-MS.

Declaration of Competing Interest

All the authors declare no conflict of interest.

References

Adem, S., Eyupoglu, V., Sarfraz, I., Rasul, A., Ali, M., 2020. Identification of potent COVID-19 main protease (Mpro) inhibitors from natural polyphenols: An in silico strategy unveils a hope against CORONA. Preprint. https://doi.org/10.20944/preprints202003.0333.v1

Agarwal, S., Kalpana, S., 1988. Anti-inflammatory activity of flowers of Rhododendron arboreum (SMITH) in rat's hind paw oedema induced by various phlogistic agents. Indian journal of pharmacology 10, 86-89.

Bernstein, F.C., Koetzle, T.F., Williams, G.J.B., Meyer, E.F., Brice, M.D., Rodgers, J.R., Kennard, O., Shimanouchi, T., Tasumi, M., 1978. The protein data bank: A computer-based archival file for macromolecular structures. Archives of Biochemistry and Biophysics 185, 584-591. https://doi.org/10.1016/0003-9861(78)90204-7

Bhandary, M.R., Kawabata, J., 2009. Antidiabetic Activity of Laligurans (Rhododendron arboreum Sm.) Flower. Journal of Food Science and Technology Nepal 4, 61-63. https://www.nepjol.info/index.php/JFSTN/article/view/2001

Bolton, E.E., Wang, Y., Thiessen, P.A., Bryant, S.H., 2008. PubChem: integrated platform of small molecules and biological activities. Annual Reports in Computational Chemistry 4, 217-241. https://doi.org/10.1016/S1574-1400(08)00012-1

Cheng, F., Li, W., Zhou, Y., Shen, J., Wu, Z., Liu, G., Lee, P.W., Tang, Y., 2012. admetSAR: A comprehensive source and free tool for assessment of chemical ADMET properties. Journal of Chemical Information and Modeling 52, 3099-3105. https://doi.org/10.1021/ci300367a

Cheng, V.C.C., Lau, S.K.P., Woo, P.C.Y., Kwok, Y.Y., 2007. Severe acute respiratory syndrome coronavirus as an agent of emerging and reemerging infection. Clinical Microbiology Reviews 20, 660-694. https://doi.org/10.1128/CMR.00023-07

Daina, A., Michielin, O., Zoete, V., 2017. SwissADME: a free web tool to evaluate pharmacokinetics, drug-likeness and medicinal chemistry friendliness of small molecules. Scientific Reports 7, 42717. https://doi.org/10.1038/srep42717

Dallakyan, S., Olson, A.J., 2015. Small-molecule library screening by docking with PyRx. Methods in Molecular Biology 1263, 243-250. https://doi.org/10.1007/978-1-4939-2269-7_19

Devi, S., Kanta Vats, C., Dhaliwal, Y., 2018. Quality Evaluation of Rhododendron arboreum Flowers of Different Regions of Himachal Pradesh for Standardization of Juice Extraction Technique. International Journal of Advances in Agricultural Science and Technology 5, 51-57.

Ding, Y., Cao, Z., Cao, L., Ding, G., Wang, Z., Xiao, W., 2017. Antiviral activity of chlorogenic acid against influenza A (H1N1/H3N2) virus and its inhibition of neuraminidase. Scientific Reports 7, 45723. https://doi.org/10.1038/srep45723

Ferreira, P.G., Ferraz, A.C., Figueiredo, J.E., Lima, C.F., Rodrigues, V.G., Taranto, A.G., Ferreira, J.M.S., Brandao, G.C., Vieira-Filho, S.A., Duarte, L.P., de Brito Magalhaes, C.L., de Magalhaes, J.C., 2018. Detection of the antiviral activity of epicatechin isolated from Salacia crassifolia (Celastraceae) against Mayaro virus based on protein C homology modelling and virtual screening. Archives of

Virology 163, 1567-1576. https://doi.org/10.1007/s00705-018-3774-1

Hagiwara, A., Miyashita, K., Nakanishi, T., Sano, M., Tamano, S., Kadota, T., Koda, T., Nakamura, M., Imaida, K., Ito, N., Shirai, T., 2001. Pronounced inhibition by a natural anthocyanin, purple corn color, of 2-amino-1-methyl-6-phenylimidazo pyridine [4,5-b] (PhIP)-associated colorectal carcinogenesis in male F344 rats pretreated with 1, 2-dimethylhydrazine. Cancer letters 171, 17-25. https://doi.org/10.1016/s0304-3835(01)00510-9

Harman, D., 2006. Free radical theory of aging: An update- Increasing the functional life span. Annals of the New York Academy of Sciences 1067, 10-21. https://doi.org/10.1196/annals.1354.003

Horby, P., Lim, W.S., Emberson, J., Mafham, M., Bell, J., Linsell, L., Staplin, N., Brightling, C., Ustianowski, A., Elmahi, E., Prudon, B., Green, C., Felton, T., Chadwick, D., Rege, K., Fegan, C., Chappell, L.C., Faust, S.N., Jaki, T., Jeffery, K., Montgomery, A., Rowan, K., Juszczak, E., Baillie, J.K., Haynes, R., Landray, M.J., Recovery Collaborative Group., 2020. Effect of dexamethasone in hospitalized patients with COVID-19: preliminary report. Preprint medRxiv. https://doi.org/10.1101/2020.06.22.20137273

Huang, C., Wang, Y., Li, X., Ren, L., Zhao, J., Hu, Y., Zhang, L., Fan, G., Xu, J., Gu, X., Cheng, Z., Yu, T., Xia, J., Wei, Y., Wu, W., Xie, X., Yin, W., Li, H., Liu, M., Xiao, Y., Gao, H., Guo, L., Xie, J., Wang, G., Jiang, R., Gao, Z., Jin, Q., Wang, J., Cao, B., 2020. Clinical features of patients infected with 2019 novel coronavirus in Wuhan, China. The Lancet 395, 497–506. https://doi.org/10.1016/S0140-6736(20)30183-5

Jena, A. B., Kanungo, N., Nayak, V., Chainy, G.B.N., Dandapat, J., 2019. Catechin and Curcumin interact with corona (2019-nCoV/SARS-CoV2) viral S protein and ACE2 of human cell membrane : insights from Computational study and implication for intervention. Preprint from Research Square. https://doi.org/10.21203/rs.3.rs-22057/v1

Jin, Z., Du, X., Xu, Y., Deng, Y., Liu, M., Zhao, Y., Zhang, B., Li, X., Zhang, L., Peng, C., Duan, Y., Yu, J., Wang, L., Yang, K., Liu, F., Jiang, R., Yang, Xinglou, You, T., Liu, Xiaoce, Yang, Xiuna, Bai, F., Liu, H., Liu, Xiang, Guddat, L., Xu, W., Xiao, G., Qin, C., Shi, Z., Jiang, H., Rao, Z., Yang, H., 2020. Structure of M pro from SARS-CoV-2 and discovery of its inhibitors. Nature 582, 289-293. https://doi.org/10.1038/s41586-020-2223-y

Khaerunnisa, S., Kurniawan, H., Awaluddin, R., Suhartati, S., Soetjipto, S., 2020. Potential inhibitor of COVID-19 main protease (Mpro) from several medicinal plant compounds by molecular docking study. Preprints 2020030226. https://doi.org/10.20944/preprints202003.0226.v1

Kim, S., Chen, J., Cheng, T., Gindulyte, A., He, J., He, S., Li, Q., Shoemaker, B.A., Thiessen, P.A., Yu, B., Zaslavsky, L., Zhang, J., Bolton, E.E., 2019. PubChem 2019 update: improved access to chemical data. Nucleic Acids Research 47, D1102-D1109. https://doi.org/10.1093/nar/gky1033

Kumar, V., Suri, S., Prasad, R., Gat, Y., Sangma, C., Jakhu, H., Sharma, M., 2019. Bioactive compounds, health benefits and utilization of Rhododendron: A comprehensive review. Agriculture and Food Security 8, 6. https://doi.org/10.1186/s40066-019-0251-3

Kupina, S., Fields, C., Roman, M.C., Brunelle, S.L., 2019. Determination of total phenolic content using the Folin-C assay: Single-laboratory validation, first action 2017.13. Journal of AOAC International 101, 1466-1472. https://doi.org/10.5740/jaoacint.18-0031

Laloo, R.C., Kharlukhi, L., Jeeva, S., Mishra, B.P., 2006. Status of medicinal plants in the disturbed and the undisturbed sacred forests of Meghalaya, Northeast India: population structure and regeneration efficacy of some important species. Current Science 90, 225-231.

Li, J., Zhou, L., Zhang, Y., 2001. Studies on the effects of tea catechins against hepatitis B virus infection. Chinese journal of preventive medicine 35, 404-407.

Li, X., Liu, Y., Hou, X., Peng, H., Zhang, Li., Jiang, Q., Shi, M., Ji, Y., Wang, Y., Shi, W., 2013. Chlorogenic Acid Inhibits the Replication and Viability of Enterovirus 71 in vitro. PLoS One 8, e76007. https://doi.org/10.1371/journal.pone.0076007

Li, Y., But, P.P.H., Ooi, V.E.C., 2005. Antiviral activity and mode of action of caffeoylquinic acids from Schefflera heptaphylla (L.) Frodin. Antiviral Research 68, 1-9. https://doi.org/10.1016/j.antiviral.2005.06.004

Lisec, J., Schauer, N., Kopka, J., Willmitzer, L., Fernie, A.R., 2006. Gas chromatography mass spectrometry-based metabolite profiling in plants. Nature Protocols 1, 387-396. https://doi.org/10.1038/nprot.2006.59

Liu, X., Wang, X.J., 2020. Potential inhibitors against 2019-nCoV coronavirus M protease from clinically approved medicines. Journal of Genetics and Genomics 47, 119-121. https://doi.org/10.1016/j.jgg.2020.02.001

Mahmood, N., Moore, P.S., De Tommasi, N., De Simone, F., Colman, S., Hay, A.J., Pizza, C., 1993. Inhibition of HIV infection by caffeoylquinic acid derivatives. Antiviral Chemistry and Chemotherapy 4, 235-240. https://doi.org/10.1177/095632029300400406

Maiti, S., Moon, U.R., Bera, P., Samanta, T., Mitra, A., 2014. The in vitro antioxidant capacities of Polianthes tuberosa L. flower extracts. Acta Physiologiae Plantarum 36, 2597-2605. https://doi.org/10.1007/s11738-014-1630-9

Malik, Y.S., Sircar, S., Bhat, S., Sharun, K., Dhama, K., Dadar, M., Tiwari, R., Chaicumpa, W., 2020. Emerging novel coronavirus (2019-nCoV)-current scenario, evolutionary perspective based on genome analysis and recent developments. Veterinary Quarterly 40, 68-76. https://doi.org/10.1080/01652176.2020.1727993

Malkoc, M., Laghari, A.Q., Kolayli, S., Can, Z., 2016. Phenolic Composition and Antioxidant Properties of Rhododendron ponticum: Traditional Nectar Source for Mad Honey. Analytical Chemistry Letters 6, 224-231. https://doi.org/10.1080/22297928.2016.1196605

Masakapalli, S.K., Bryant, F.M., Kruger, N.J., Ratcliffe, R.G., 2014a. The metabolic flux phenotype of heterotrophic Arabidopsis cells reveals a flexible balance between the cytosolic and plastidic contributions to carbohydrate oxidation in response to phosphate limitation. The Plant Journal 78, 964-977. https://doi.org/10.1111/tpj.12522

Masakapalli, S.K., Ratcliffe, R.G., Williams, T.C.R., 2014b. Quantification of 13 C enrichments and isotopomer abundances for metabolic flux analysis using 1D NMR spectroscopy. Plant Metabolic Flux Analysis: Methods and Protocols, Methods in Molecular Biology 1090, 73-86. https://doi.org/10.1007/978-1-62703-688-7_5

Min, S.W., Ryu, S.N., Kim, D.H., 2010. Anti-inflammatory effects of black rice, cyanidin-3-O-β-d-glycoside, and its metabolites, cyanidin and protocatechuic acid. International Immunopharmacology 10, 959-966. https://doi.org/10.1016/j.intimp.2010.05.009

Pandit, M., Latha, N., 2020. In silico studies reveal potential antiviral activity of phytochemicals from medicinal plants for the treatment of COVID-19 infection. Preprint from Research square. https://doi.org/10.21203/rs.3.rs-22687/v1

Pires, D.E.V., Blundell, T.L., Ascher, D.B., 2015. pkCSM: Predicting small-molecule pharmacokinetic and toxicity properties using graph-based signatures. Journal of Medicinal Chemistry 58, 4066-4072. https://doi.org/10.1021/acs.jmedchem.5b00104

Ren, J., Huang, J., Yang, B., Lin, S., Li, J., Liao, H., Yuan, X., Wu, X., Ou, S., 2019. Docking and molecular dynamics: simulation of the inhibition of H5N1 influenza virus (Anhui 2005) neuraminidase (NA) by chlorogenic acid (CHA). International Journal of Clinical and Experimental Medicine 12, 9815-9823.

Serina, J.C., Castilho, P.C., Fernandes, M.X., 2017. Caffeoylquinic acids as inhibitors for HIV-I protease and HIV-I Integrase. A Molecular docking study. Journal of Computational Chemistry & Molecular Modelling 1, 34-37. https://doi.org/10.25177/jccmm.1.2.1

Shree, M., Lingwan, M., Masakapalli, S.K., 2019. Metabolite Profiling and Metabolomics of Plant Systems Using 1H NMR and GC-MS. OMICS-Based Approaches in Plant Biotechnology. 129, 129-144. https://doi.org/10.1002/9781119509967.ch7

Shrestha, A., 2016. Phytochemical Analysis of Rhododendron Species. Doctoral dissertation, IRC-Library, Information Resource Center der Jacobs University Bremen.

Solaimanzadeh, I., 2020. Acetazolamide, Nifedipine and Phosphodiesterase Inhibitors: Rationale for Their Utilization as Adjunctive Countermeasures in the Treatment of Coronavirus Disease 2019 (COVID-19). Cureus 12, e7343. https://doi.org/10.7759/cureus.7343

Sonar, P.K., Singh, R., Khan, S., Saraf, S.K., 2012. Isolation, characterization and activity of the flowers of Rhododendron arboreum (Ericaceae). Journal of Chemistry 9, 631-636. https://doi.org/10.1155/2012/872147

Song, J.M., Lee, K.H., Seong, B.L., 2005. Antiviral effect of catechins in green tea on influenza virus. Antiviral Research 68, 66-74. https://doi.org/10.1016/j.antiviral.2005.06.010

Thangaraj, V., 2013. Hypolipidemic effect of Rhododendron arboreum Sm. linn flower juice in experimentally induced hypercholestermic rabbits. Int J Pharm Biomed Res. 4, 46-49.

Srivastava, P., 2012. Rhododendron arboreum: an overview. Journal of Applied Pharmaceutical Science 2, 158-162.

Tian, W., Chen, C., Lei, X., Zhao, J., Liang, J., 2018. CASTp 3.0: Computed atlas of surface topography of proteins. Nucleic Acids Research 46, W363-W367. https://doi.org/10.1093/nar/gky473

Towler, P., Staker, B., Prasad, S.G., Menon, S., Tang, J., Parsons, T., Ryan, D., Fisher, M., Williams, D., Dales, N.A., Patane, M.A., Pantoliano, M.W., 2004. ACE2 X-Ray Structures Reveal a Large Hinge-bending Motion Important for Inhibitor Binding and Catalysis. Journal of Biological Chemistry 279, 17996-18007. https://doi.org/10.1074/jbc.M311191200

Tsuda, T., Horio, F., Uchida, K., Aoki, H., Osawa, T., 2003. Dietary Cyanidin 3-O-β-D-Glucoside-Rich Purple Corn Color Prevents Obesity and Ameliorates Hyperglycemia in Mice. The Journal of Nutrition 133, 2125-2130. https://doi.org/10.1093/jn/133.7.2125

Tsuda, T., Watanabe, M., Ohshima, K., Norinobu, S., Choi, S.W., Kawakishi, S., Osawa, T., 1994. Antioxidative Activity of the Anthocyanin Pigments Cyanidin 3-O-β-d-Glucoside and Cyanidin. Journal of Agricultural and Food Chemistry 42, 2407-2410. https://doi.org/10.1021/jf00047a009

Uniyal, S.K., Singh, K.N., Jamwal, P., Lal, B., 2006. Traditional use of medicinal plants among the tribal communities of Chhota Bhangal, Western Himalaya. Journal of Ethnobiology and Ethnomedicine 2, 14. https://doi.org/10.1186/1746-4269-2-14

Urushisaki, T., Takemura, T., Tazawa, S., Fukuoka, M., Hosokawa-Muto, J., Araki, Y., Kuwata, K., 2011. Caffeoylquinic Acids Are Major Constituents with Potent Anti-Influenza Effects in Brazilian Green Propolis Water Extract. Evid. Based Complement Alternat Med. 2011, 254914 https://doi.org/10.1155/2011/254914

Verma, N., Singh, A.P., Amresh, G., Sahu, P.K., Rao, C.V., 2011. Protective effect of ethyl acetate fraction of Rhododendron arboreum flowers against carbon tetrachloride-induced hepatotoxicity in experimental models. Indian Journal of Pharmacology 43, 291-295. https://doi.org/10.4103/0253-

7613.81518

Wan, Y., Shang, J., Graham, R., Baric, R.S., Li, F., 2020. Receptor Recognition by the Novel Coronavirus from Wuhan: an Analysis Based on Decade-Long Structural Studies of SARS Coronavirus. Journal of Virology 94, e00127-20. https://doi.org/10.1128/jvi.00127-20

Wang, G.F., Shi, L.P., Ren, Y.D., Liu, Q.F., Liu, H.F., Zhang, R.J., Li, Z., Zhu, F.H., He, P.L., Tang, W., Tao, P.Z., Li, C., Zhao, W.M., Zuo, J.P., 2009. Anti-hepatitis B virus activity of chlorogenic acid, quinic acid and caffeic acid in vivo and in vitro. Antiviral Research 83, 186-190. https://doi.org/10.1016/j.antiviral.2009.05.002

Yadav, A., Lingwan, M., Yadukrishnan, P., Masakapalli, S.K., Datta, S., 2019. BBX31 promotes hypocotyl growth, primary root elongation and UV-B tolerance in Arabidopsis. Plant signaling and behavior 14, e1588672. https://doi.org/10.1080/15592324.2019.1588672

Yazdi, S.E., Prinsloo, G., Heyman, H.M., Oosthuizen, C.B., Klimkait, T., Meyer, J.J.M., 2019. Anti-HIV-1 activity of quinic acid isolated from Helichrysum mimetes using NMR-based metabolomics and computational analysis. South African Journal of Botany 126, 328-339. https://doi.org/10.1016/j.sajb.2019.04.023

Zanello, P.R., Koishi, A.C., Rezende, C.D.O., de Oliveira, L.A., Pereira, A.A., de Almeida, M.V., Duarte Dos Santos, C.N., Bordignon, J., 2015. Quinic acid derivatives inhibit dengue virus replication in vitro. Virology Journal 12, 1-13. https://doi.org/10.1186/s12985-015-0443-9

Zell, S.G., Goodman, P.H., 1988. Acetazolamide and dexamethasone in the prevention of acute mountain sickness. Western Journal of Medicine 148, 541–545.

Zhang, J.J., Shen, X., Yan, Y.M., Wang, Y., Cheng, Y.X., 2020. Discovery of anti-SARS-CoV-2 agents from commercially available flavor via docking screening. Preprint. 1-27. https://doi.org/10.31219/osf.io/vjch2

Preprints (www.preprints.org) | NOT PEER-REVIEWED | Posted: 24 August 2020 doi:10.20944/preprints202008.0530.v1

625 **Tables**

626 **Table 1.** Active site docking of *R. arboreum* petal phytochemicals against SARS-CoV-2 Mpro (6LU7)
627 showing the binding affinities and interacting amino acid residues

***R. arboreum* petal Phytochemicals**	**SARS-CoV-2 M^{pro} (6LU7)**	
	Binding affinity (Kcal/mol)	**Interacting Amino acid Residues**
Epicatechin gallate	-7.3	THRA:24, THRA:25, THRA:26, LEUA:27, HISA:41, VALA:42, META:49, PHEA:140, LEUA:141, ASNA:142, GLYA:143, SERA:144, CYSA:145, GLUA:166, META:165, HISA:163, HISA:164, HISA:172, GLNA:189
5-O-Feruloylquinic acid	-7.2	THRA:25, THRA:26, LEUA:27, HISA:41, META:49, PHEA:140, LEUA:141, ASNA:142, GLYA:143, SERA:144, CYSA:145, HISA:164, GLUA:166, META:165, HISA:163, HISA:172, GLNA:189
Quercetin-O-rhamnoside	-7.2	THRA:25, THRA:26, LEUA:27, HISA:41, VALA:42, META:49, PHEA:140, LEUA:141, ASNA:142, GLYA:143, CYSA:145, GLUA:166, META:165, HISA:163, HISA:172, GLNA:189
5-O-Coumaroyl-D-quinic acid	-7.2	THRA:25, THRA:26, LEUA:27, HISA:41, META:49, PHEA:140, LEUA:141, ASNA:142, GLYA:143, SERA:144, CYSA:145 GLUA:166, META:165, HISA:164, HISA:163, HISA:172, GLNA:189
3-Caffeoyl-quinic acid	-7.1	THRA:24, THRA:25, THRA:26, LEUA:27, HISA:41, THRA:45, META:49, PHEA:140, LEUA:141, ASNA:142, GLYA:143, SERA:144, CYSA:145, GLUA:166, META:165, HISA:163, HISA:164, HISA:172
Quercetin-O-pentoside	-7.1	THRA:24, THRA:25, THRA:26, LEUA:27, META:49, PHEA:140, LEUA:141, ASNA:142, GLYA:143, SERA:144, CYSA:145, GLUA:166, META:165, HISA:163, HISA:172, GLNA:189
Kaempferol	-7.1	THRA:25, THRA:26, LEUA:27, HISA:41, PHEA:140, LEUA:141, ASNA:142, GLYA:143, SERA:144, CYSA:145, GLUA:166, META:165, HISA:163, HISA:172, GLNA:189
Kaempferol-O-pentoside	-7.0	THRA:24, THRA:25, THRA:26, LEUA:27, META:49, PHEA:140, LEUA:141, ASNA:142, GLYA:143, SERA:144, CYSA:145, GLUA:166, META:165, HISA:163, HISA:164, HISA:172, GLNA:189
Epicatechin	-7.0	PHEA:140, LEUA:141, SERA:144, GLYA:143, ASNA:142, CYSA:145, GLNA:189, HISA:163, META:165, GLUA:166, LEUA:167, PROA:168
Quercetin	-7.0	THRA:25, THRA:26, LEUA:27, HISA:41, PHEA:140, LEUA:141, ASNA:142, GLYA:143, SERA:144, CYSA:145 GLUA:166, META:165, HISA:163, HISA:172, GLNA:189
Catechin	-6.7	THRA:25, THRA:26, LEUA:27, HISA:41, META:49, PHEA:140, LEUA:141, ASNA:142, GLYA:143, SERA:144, CYSA:145, GLUA:166, META:165, HISA:163, HISA:172

Preprints (www.preprints.org) | NOT PEER-REVIEWED | Posted: 24 August 2020 doi:10.20944/preprints202008.0530.v1

Caffeic acid	-5.7	PHEA:140, LEUA:141, ASNA:142, GLYA:143, SERA:144, CYSA:145, GLUA:166, META:165, HISA:163, GLNA:189
Protocatechuic acid	-5.4	PHEA:140, LEUA:141, ASNA:142, GLYA:143, SERA:144, CYSA:145, GLNA:189, GLUA:166, HISA:163, META:165
Quinic acid	-5.4	LEUA:141, ASNA:142, GLYA:143, SERA:144, CYSA:145, HISA:163, META:165, GLUA:166, GLNA:189
2,4-Quinolinediamine	-5.1	HISA:41, META:49, GLNA:189, CYSA:145, HISA:164, META:165, GLUA:166, HISA:163, ASNA:142, LEUA:141, GLYA:143
4-Coumaric acid	-5.1	PHEA:140, LEUA:141, ASNA:142, HISA:163, SERA:144, GLYA:143, CYSA:145, META:165, GLUA:166, LEUA:167, GLNA:189
3-Hydroxybenzoic acid	-4.9	PHEA:140, LEUA:141, ASNA:142, GLYA:143, SERA:144, CYSA:145, , GLUA:166, HISA:163, HISA:172
Shikimic acid	-5.3	PHEA:140, LEUA:141, ASNA:142, GLYA:143, SERA:144, CYSA:145, GLUA:166, HISA:163, META:165, HISA:172,
Glycyrrhizic acid (Positive control) (Zhang et al., 2020)	-7.2	PHEA:140, LEUA:141, SERA:139, HISA:172, GLYA:138, LYSA:137, TYRA:118, SERA:123, ALAA:116, GLYA:124, TYRA:126, VALA:125, GLUA:290, LYSA:5

Table 2. Active site docking of *R. arboreum* petal phytochemicals against Human Angiotensin Converting Enzyme ACE2 (1R4L) showing the binding affinities and interacting amino acid residues

***R. arboreum* petal Phytochemicals**	**Human Angiotensin Converting Enzyme (1R4L)**	
	Binding affinity (Kcal/mol)	**Interacting Amino acid Residues**
Quercetin-O-rhamnoside	-10.2	GLUA:406, SERA:409, LEUA:370, ASPA:367, THRA:276, META:270, ASNA:149, TRPA:271, ASPA:269, PHEA:274, HISA:345, PROA:346, HISA:505, ARGA:273, TYRA:515, GLUA:375, THRA:371, ARGA:518, HISA:374
Epicatechin gallate	-10.1	ALAA:153, ASNA:149, TRPA:271, HISA:345, ARGA:273, HISA:505, PROA:346, THRA:347, GLUA:375, TYRA:515, GLUA:402, HISA:378, HISA:374, THRA:371, ARGA:518, PHEA:274, THRA:445, THRA:276, ASPA:367, ASPA:269
Quercetin-O-pentoside	-9.9	TRPA:271, ARGA:273, THRA:371, HISA:505, TYRA:515, GLUA:402, HISA:374, HISA:378, GLUA:375, THRA:347, ARGA:518, PROA:346, GLUA:406, THRA:445, ASPA:367, THRA:276, PHEA:274, HISA:345
Kaempferol-O-pentoside	-9.7	GLUA:406, SERA:409, ARGA:518, HISA:374, THRA:347, HISA:505, GLUA:375, HISA:378, GLUA:402, TYRA:515, ARGA:273, THRA:371, HISA:345, PROA:346, PHEA:274, ASPA:367, THRA:276, THRA:445
Catechin	-9.0	PROA:346, THRA:347, HISA:345, GLUA:375, THRA:371, PHEA:274, ASPA:269, ASPA:367, THRA:276, THRA:445, LEUA:370, GLUA:406, ARGA:518, ARGA:273, TYRA:515, GLUA:402, HISA:505, HISA:378, HISA:374
Quercetin	-8.9	PHEA:504, HISA:505, GLUA:375, HISA:345, ARGA:273,

Preprints (www.preprints.org) | NOT PEER-REVIEWED | Posted: 24 August 2020 doi:10.20944/preprints202008.0530.v1

		THRA:371, PROA:346, PHEA:274, ARGA:518, GLUA:402, TYRA:515, HISA:374, HISA:378, TYRA:510, THRA:347, ALAA:348
5-O-Feruloylquinic acid	-8.6	ARGA:518, GLUA:406, THRA:371, ASPA:367, ARGA:273, ASPA:368, ASNA:277, ASNA:158, THRA:365, ALAA:153, LYSA:363, GLUA:145, ASNA:149, TRPA:271, ASPA:269, THRA:276, THRA:445, PHEA:274
3-Caffeoyl-quinic acid	-8.5	PROA:346, HISA:378, ARGA:273, GLUA:375, TRPA:271, HISA:345, TYRA:127, CYSA:344, GLUA:145, ASNA:149, LYSA:363, META:360, ASPA:368, THRA:371, PHEA:274, ARGA:518, HISA:374, TYRA:515, GLUA:402
5-O-Coumaroyl-D-quinic acid	-8.5	ASPA:367, THRA:276, LYSA:441, THRA:445, TYRA:515, HISA:505, HISA:374, HISA:345, HISA:378, GLUA:375, ARGA:514, GLUA:402, PROA:346, THRA:371, ARGA:518, PHEA:274, ARGA:273, LEUA:370
Epicatechin	-8.4	PROA:346, HISA:345, GLUA:375, THRA:371, PHEA:274, ASPA:367, THRA:276, THRA:445, LEUA:370, GLUA:406, ARGA:518, ARGA:273, GLUA:402, HISA:505, HISA:374
Kaempferol	-8.4	PHEA:274, HISA:505, HISA:345, ARGA:273, PROA:346, GLUA:402, HISA:378, HISA:374, GLUA:375, TYRA:515, ARGA:518, THRA:371, GLUA:406, LEUA:370, SERA:409, THRA:445
Quinic acid	-6.5	ALAA:348, GLUA:402, HISA:378, ARGA:514, TYRA:515, HISA:505, TYRA:510, PHEA:504, HISA:345, THRA:347, GLUA:375, HISA:374, PROA:346
Caffeic acid	-6.4	THRA:371, ARGA:518, ASPA:367, LEUA:370, GLUA:406, THRA:445, PHEA:274, GLNA:522, THRA:519, ILEA:446, THRA:449
2,4-Quinolinediamine	-6.3	ALAA:348, TYRA:510, TRPA:349, THRA:347, HISA:345, PHEA:504, TYRA:515, ARGA:514, HISA:505, GLUA:402, HISA:378
4-Coumaric acid	-6.2	PHEA:32, PHEA:40 LEUA:73, TRPA:69, ASPA:350, LEUA:351, PHEA:390, LEUA:391, ASNA:394, GLYA:352, ARGA:393
Shikimic acid	-6.0	ARGA:514, GLUA:402, TYRA:510, PHEA:504, THRA:347, GLUA:375, HISA:374, PROA:346, HISA:505, HISA:345, ARGA:273, TYRA:515, HISA:378
Protocatechuic acid	-5.8	ALAA:348, GLUA:402, HISA:378, ARGA:514, TYRA:515, HISA:505, TYRA:510, PHEA:504, HISA:345, ALAA:348
3-Hydroxybenzoic acid	-5.7	ARGA:514, GLUA:402, TYRA:510, PHEA:504, THRA:347, GLUA:375, HISA:374, PROA:346, HISA:505, HISA:345, ARGA:273, TYRA:515, HISA:378
Glycyrrhizic acid (Positive control) (Zhang et al., 2020)	-10.5	SERA:511, TRPA:203, TYRA:510, TYRA:199, ARGA:514, GLUA:398, ASPA:206, ASPA:509, LYSA:562, HISA:401, GLUA:402, ASNA:394, HISA:378, ASPA:350, PHEA:40, TRPA:69, PHEA:390 PHEA:32, LEUA:391, ALAA:99, LEUA:73, TRPA:202, TYRA:385

631

632

633

Preprints (www.preprints.org) | NOT PEER-REVIEWED | Posted: 24 August 2020 doi:10.20944/preprints202008.0530.v1

Figures

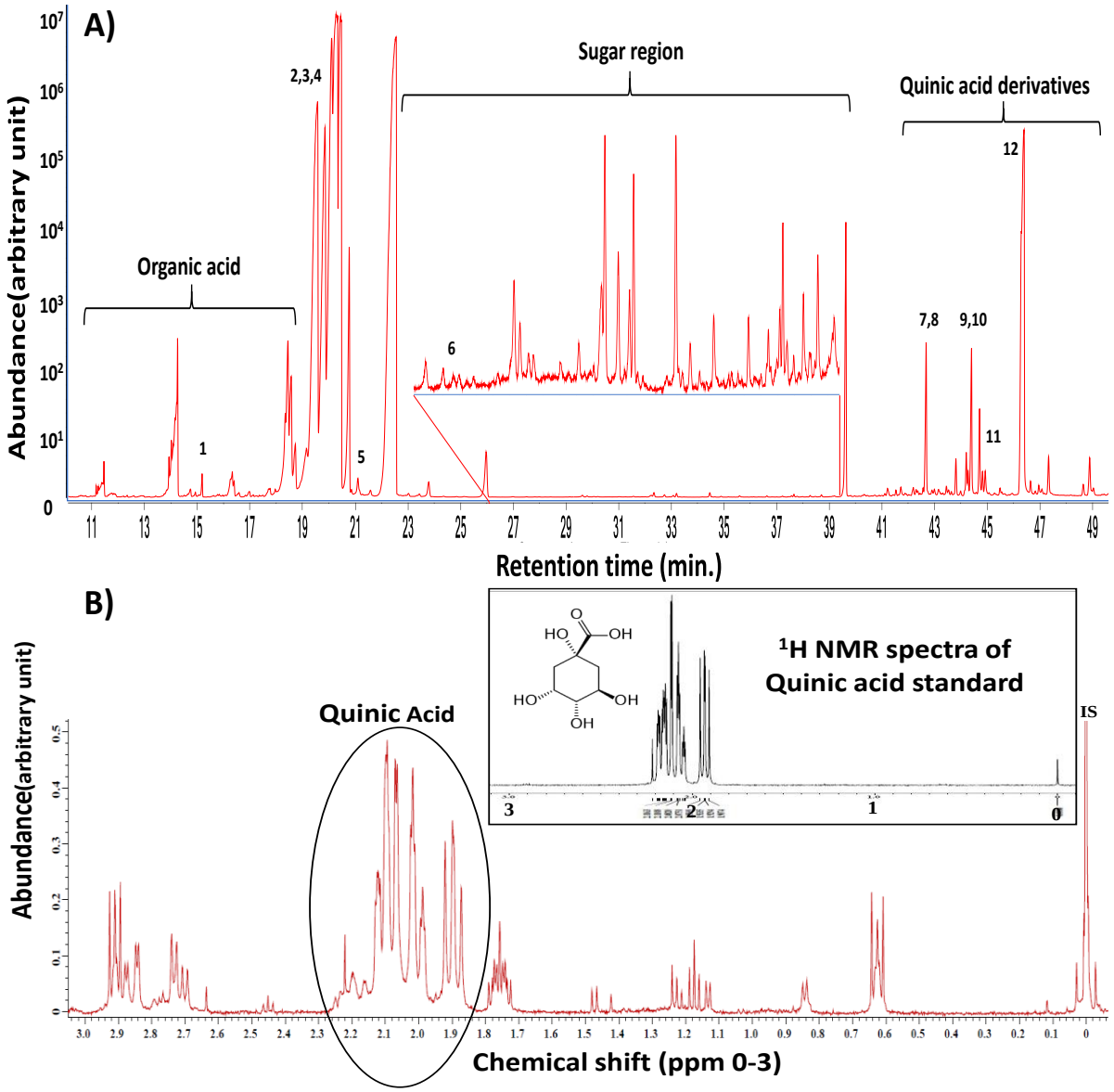

Fig. 1. Phytochemical profiles of *Rhododendron arboreum* petals. A) GC-MS spectra of hot water extract showed high abundance of secondary metabolites (~32% peak area) along with sugars, amino and organic acids. The secondary metabolites profiled are 1. Hydroxybenzoic acid 2. Shikimic acid 3. Protocatechuic acid 4. Quinic acid 5. Coumaric acid 6. Caffeic acid 7. Epicatechin 8. Catechin 9. 5-O-Coumaroyl-D-quinic acid 10. 3-Caffeoyl-quinic acid 11. 2,4-Quinolinediamine, and 12. 5-O-Feruloylquinic acid. Further metabolite profile details are presented in Supplementary Table S1 B) ^{1}H-NMR showed higher levels of quinic acid and its potential derivatives.

Preprints (www.preprints.org) | NOT PEER-REVIEWED | Posted: 24 August 2020 doi:10.20944/preprints202008.0530.v1

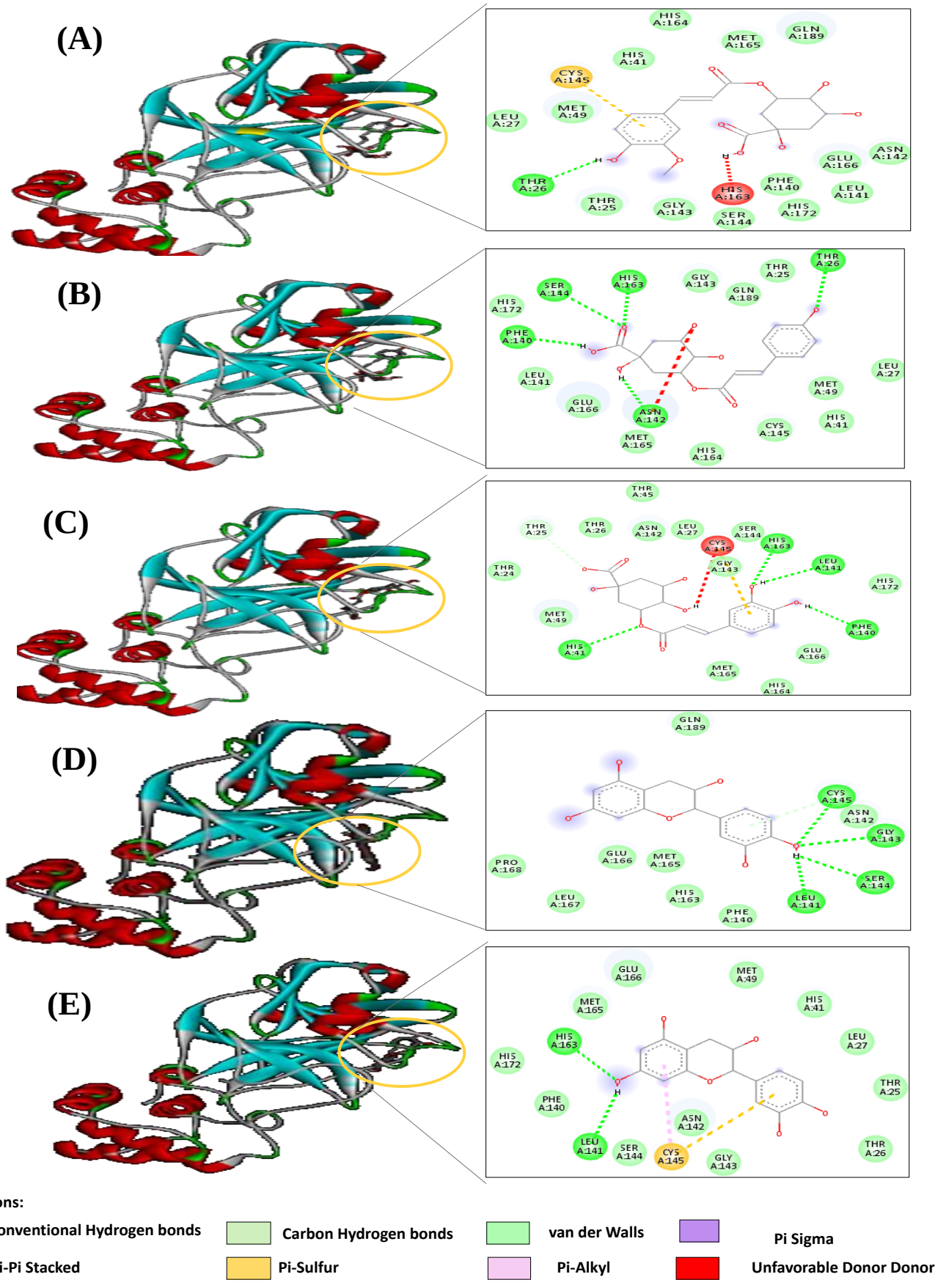

643

644 **Fig. 2.** Active site docking simulation of the interaction between SARS-CoV-2 main protease (PDB

 doi:10.20944/preprints202008.0530.v1

ID-6LU7) and (A) 5-O-Feruloylquinic acid resulted in binding affinity of -7.2 kcal/mol. The analysis showed interaction of following active site amino acid residues - THRA:25, THRA:26, LEUA:27, HISA:41, META:49, PHEA:140, LEUA:141, ASNA:142, GLYA:143, SERA:144, CYSA:145, HISA:164, GLUA:166, META:165, HISA:163, HISA:172, GLNA:189 (B) 5-O-Coumaroyl-D-quinic acid resulted in binding affinity of -7.2 kcal/mol. The analysis showed interaction of following active site amino acid residues - THRA:25, THRA:26, LEUA:27, HISA:41, META:49, PHEA:140, LEUA:141, ASNA:142, GLYA:143, SERA:144, CYSA:145 GLUA:166, META:165, HISA:164, HISA:163, HISA:172, GLNA:189 (C) 3-Caffeoyl-quinic acid resulted in binding affinity of -7.1 kcal/mol. The analysis showed interaction of following active site amino acid residues - THRA:24, THRA:25, THRA:26, LEUA:27, HISA:41, THRA:45, META:49, PHEA:140, LEUA:141, ASNA:142, GLYA:143, SERA:144, CYSA:145, GLUA:166, META:165, HISA:163, HISA:164, HISA:172 (D) Epicatechin resulted in binding affinity of -7 kcal/mol. The analysis showed interaction of following active site amino acid residues - PHEA:140, LEUA:141, SERA:144, GLYA:143, ASNA:142, CYSA:145, GLNA:189, HISA:163, META:165, GLUA:166, LEUA:167, PROA:168 (E) Catechin resulted in binding affinity of -6.7 kcal/mol. The analysis showed interaction of following active site amino acid residues - THRA:25, THRA:26, LEUA:27, HISA:41, META:49, PHEA:140, LEUA:141, ASNA:142, GLYA:143, SERA:144, CYSA:145, GLUA:166, META:165, HISA:163, HISA:172

Preprints (www.preprints.org) | NOT PEER-REVIEWED | Posted: 24 August 2020 doi:10.20944/preprints202008.0530.v1

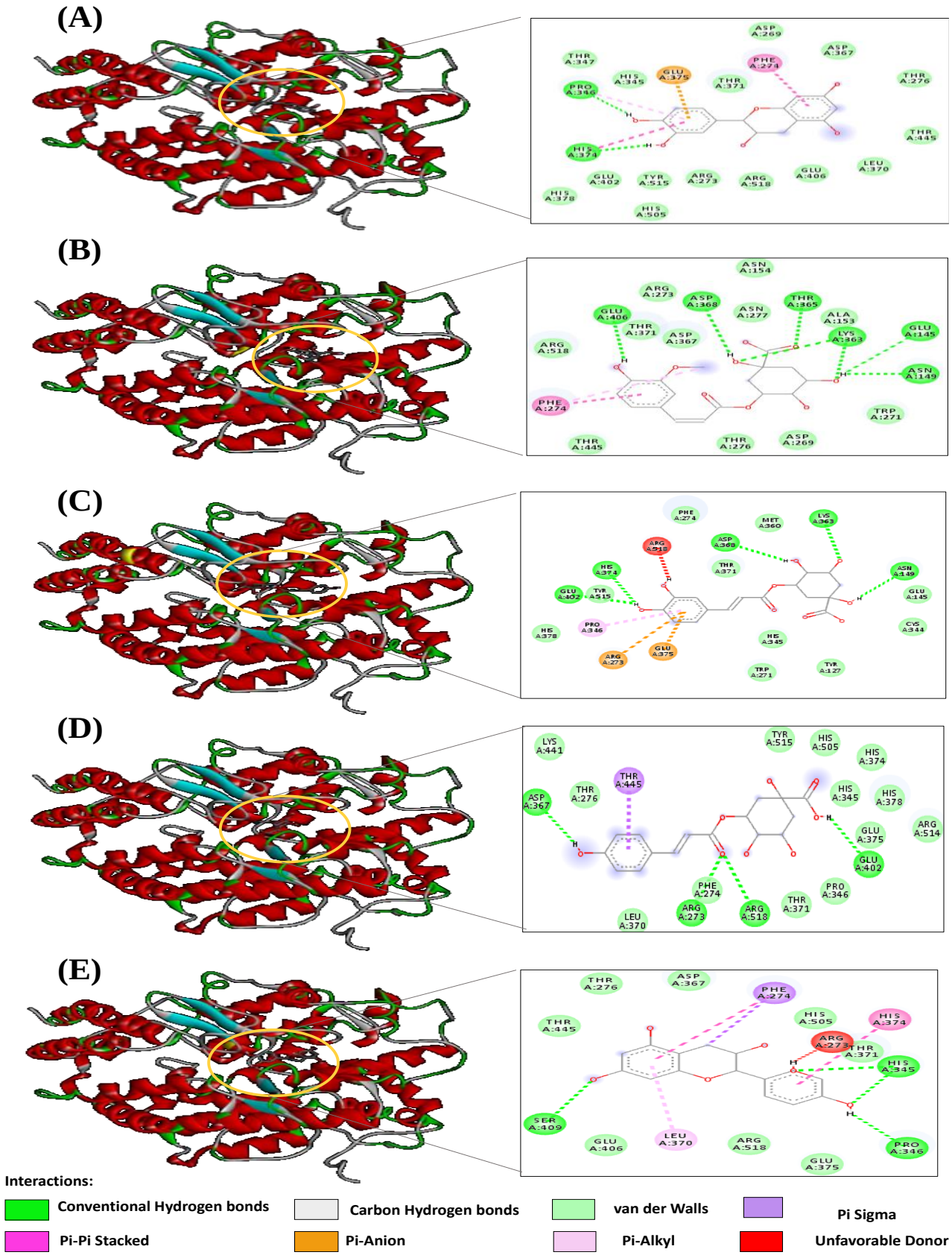

Fig. 3. Active site docking simulation of the interaction between ACE2 host cell receptor (PDB ID-1R4L) and (A) Catechin resulted in binding affinity of -9 kcal/mol. The analysis showed interaction of

 doi:10.20944/preprints202008.0530.v1

following active site amino acid residues - PROA:346, THRA:347, HISA:345, GLUA:375, THRA:371, PHEA:274, ASPA:269, ASPA:367, THRA:276, THRA:445, LEUA:370, GLUA:406, ARGA:518, ARGA:273, TYRA:515, GLUA:402, HISA:505, HISA:378, HISA:374 (B) 5-O-Feruloylquinic acid resulted in binding affinity of -8.6 kcal/mol. The analysis showed interaction of following active site amino acid residues - ARGA:518, GLUA:406, THRA:371, ASPA:367, ARGA:273, ASPA:368, ASNA:277, ASNA:158, THRA:365, ALAA:153, LYSA:363, GLUA:145, ASNA:149, TRPA:271, ASPA:269, THRA:276, THRA:445, PHEA:274 (C) 3-Caffeoyl-quinic acid resulted in binding affinity of -8.5 kcal/mol. The analysis showed interaction of following active site amino acid residues - PROA:346, HISA:378, ARGA:273, GLUA:375, TRPA:271, HISA:345, TYRA:127, CYSA:344, GLUA:145, ASNA:149, LYSA:363, META:360, ASPA:368, THRA:371, PHEA:274, ARGA:518, HISA:374, TYRA:515, GLUA:402 (D) 5-O-Coumaroyl-D-quinic acid resulted in binding affinity of -8.5 kcal/mol. The analysis showed interaction of following active site amino acid residues - ASPA:367, THRA:276, LYSA:441, THRA:445, TYRA:515, HISA:505, HISA:374, HISA:345, HISA:378, GLUA:375, ARGA:514, GLUA:402, PROA:346, THRA:371, ARGA:518, PHEA:274, ARGA:273, LEUA:370 (E) Epicatechin resulted in binding affinity of -8.4 kcal/mol. The analysis showed interaction of following active site amino acid residues -PROA:346, HISA:345, GLUA:375, THRA:371, PHEA:274, ASPA:367, THRA:276, THRA:445, LEUA:370, GLUA:406, ARGA:518, ARGA:273, GLUA:402, HISA:505,, HISA:374.

Preprints (www.preprints.org) | NOT PEER-REVIEWED | Posted: 24 August 2020 doi:10.20944/preprints202008.0530.v1

699 **Supplementary Figures**

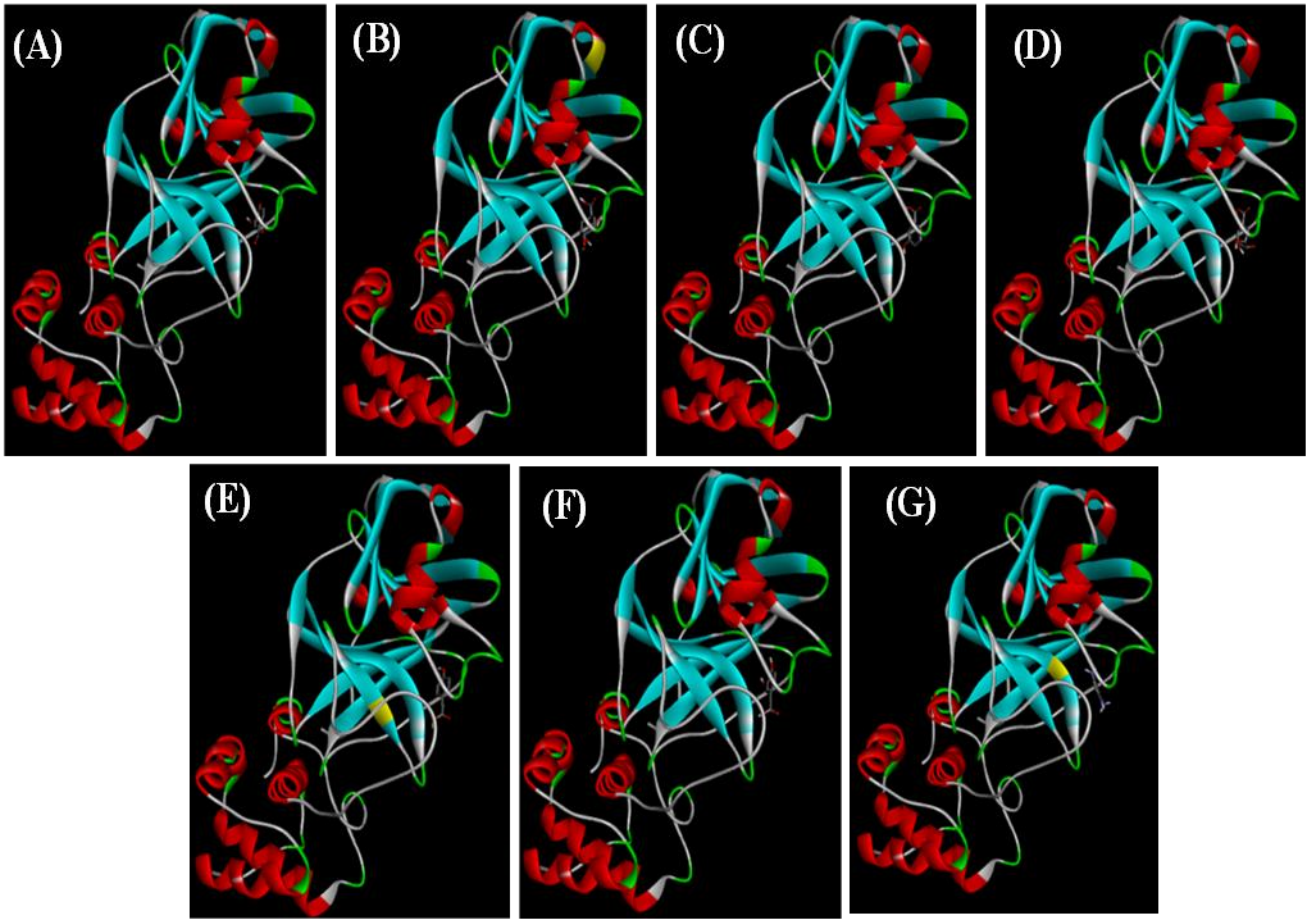

700

701 **Fig. S1.** Active site docking analysis visualisation of SARS-CoV-2 main protease (6LU7) binding with
702 (A) Protocatechuic acid (binding affinity: -5.4 kcal/mol), (B) Quinic acid (binding affinity: -5.4
703 kcal/mol), (C) 3-Hydroxybenzoic acid (binding affinity: -4.9 kcal/mol), (D) Shikimic acid (binding
704 affinity: -5.3 kcal/mol), (E) 4-Coumaric acid (binding affinity: -5.1 kcal/mol), (F) Caffeic acid (binding
705 affinity: -5.7 kcal/mol), (G) 2,4-Quinolinediamine (binding affinity: -5.1 kcal/mol). Docking of the
706 *Rhododendron* molecules against the target proteins was done using the PyRx software and analyses of
707 the docking results were carried out by using the software Biovia Discovery studio client 2020.

Preprints (www.preprints.org) | NOT PEER-REVIEWED | Posted: 24 August 2020 doi:10.20944/preprints202008.0530.v1

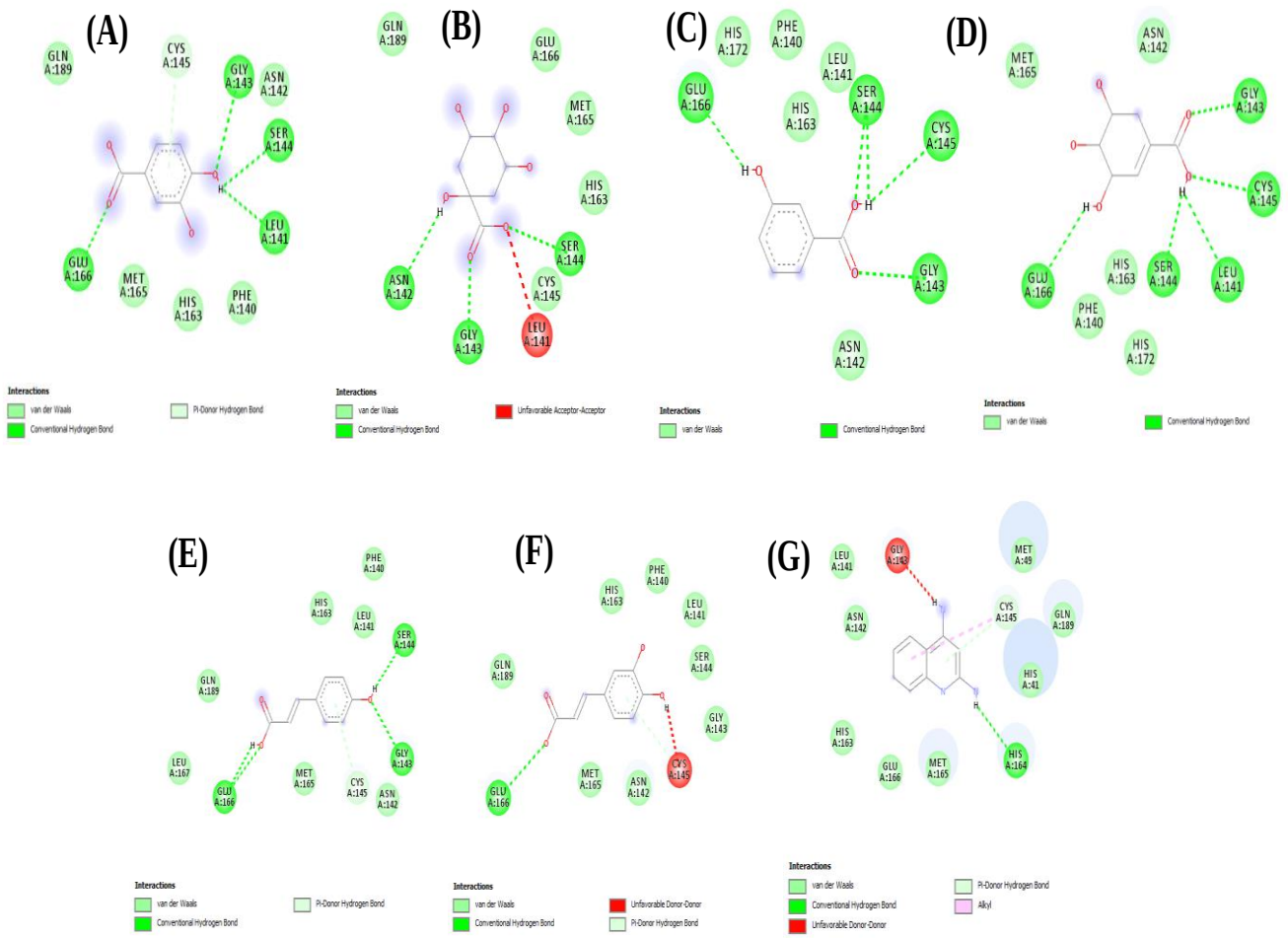

Fig. S2. Amino acid residue interactions of 6LU7 binding with ((A) Protocatechuic acid, (B) Quinic acid (C) 3-Hydroxybenzoic acid (D) Shikimic acid, (E) 4-Coumaric acid, (F) Caffeic acid, (G) 2,4-Quinolinediamine

Preprints (www.preprints.org) | NOT PEER-REVIEWED | Posted: 24 August 2020 doi:10.20944/preprints202008.0530.v1

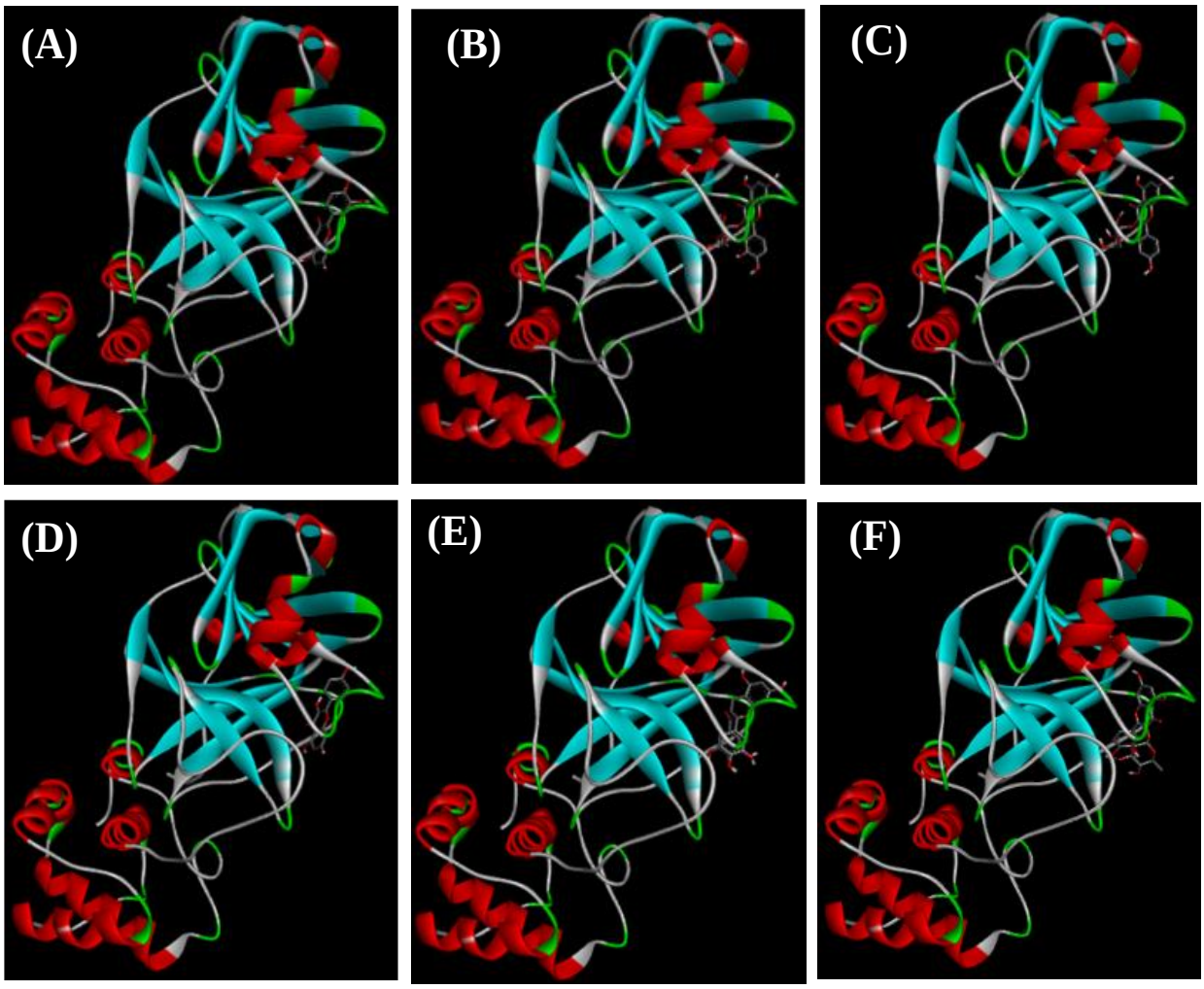

Fig. S3. Active site docking analysis visualisation of SARS-CoV-2 main protease (6LU7) binding with (A) Quercetin (binding affinity: -7 kcal/mol), (B) Quercetin-O-pentoside (binding affinity: -7.1 kcal/mol), (C) Kaempferol-O-pentoside (binding affinity: -7 kcal/mol), (D) Kaempferol (binding affinity: -7.1 kcal/mol), (E) Epicatechin gallate (binding affinity: -7.3 kcal/mol), (F) Quercetin-O-rhamnoside (binding affinity: -7.2 kcal/mol). Docking of the *Rhododendron* molecules against the target proteins was done using the PyRx software and analyses of the docking results were carried out by using the software Biovia Discovery studio client 2020.

Preprints (www.preprints.org) | NOT PEER-REVIEWED | Posted: 24 August 2020 doi:10.20944/preprints202008.0530.v1

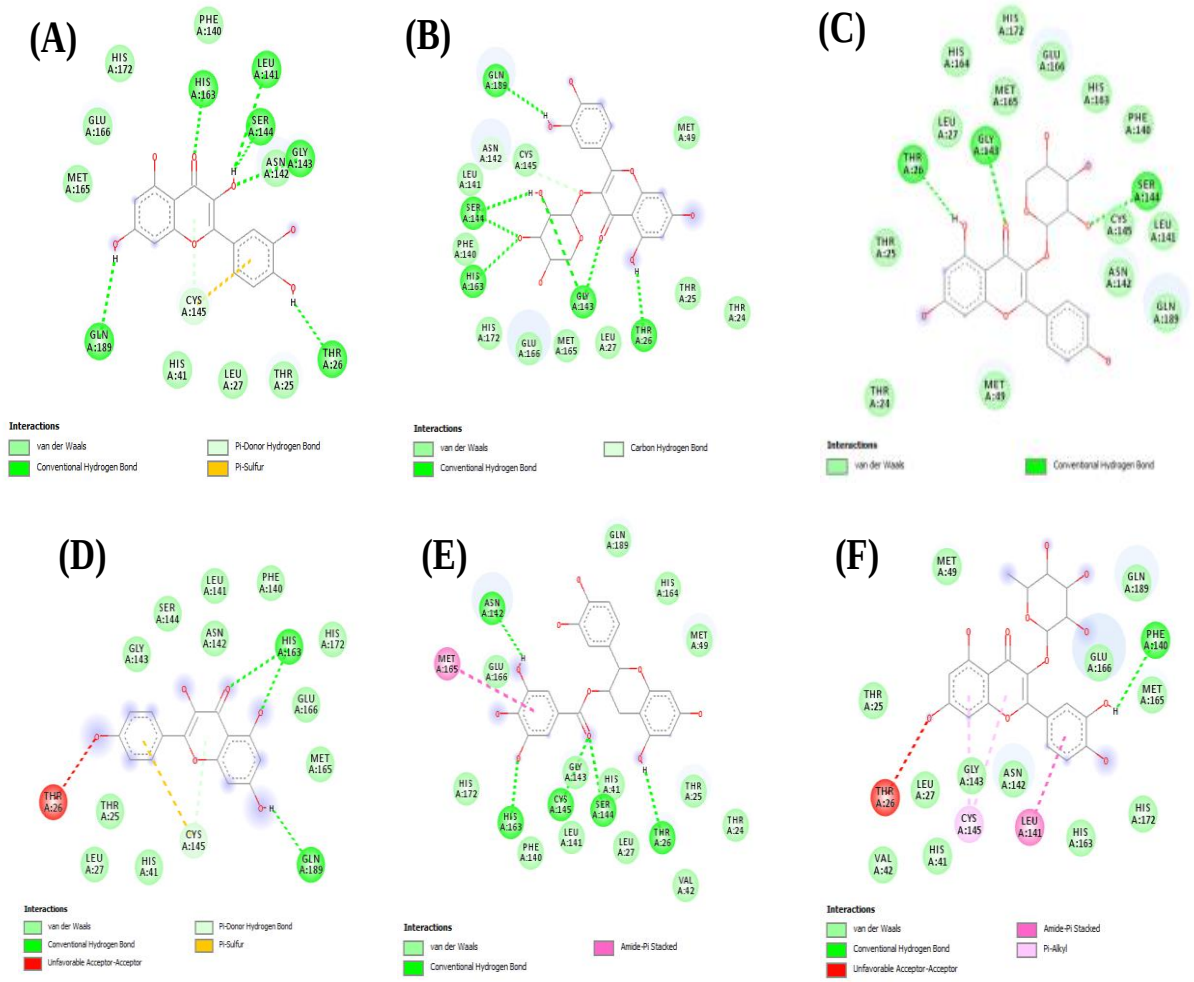

Fig. S4. Amino acid residue interactions of 6LU7 binding with (A) Quercetin (B) Quercetin-O-pentoside (C) Kaempferol-O-pentoside (D) Kaempferol (E) Epicatechin gallate (F) Quercetin-O-rhamnoside.

Preprints (www.preprints.org) | NOT PEER-REVIEWED | Posted: 24 August 2020 doi:10.20944/preprints202008.0530.v1

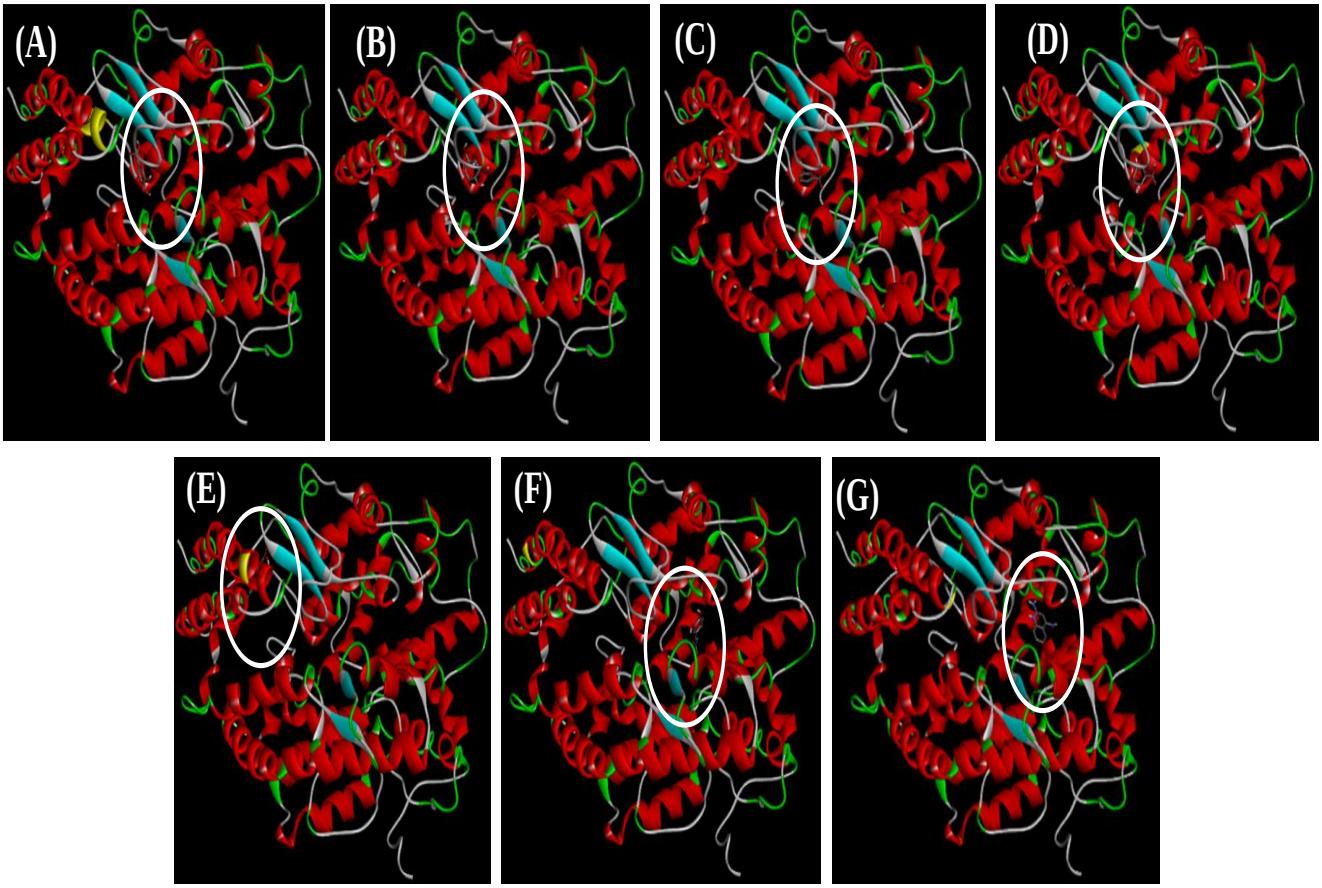

Fig. S5. Active site docking simulation of the interaction between ACE2 host cell receptor (PDB ID-1R4L) and (A) Protocatechuic acid (binding affinity: -5.8 kcal/mol), (B) Quinic acid (binding affinity: -6.5 kcal/mol), (C) 3- Hydroxybenzoic acid (binding affinity: -5.7 kcal/mol), (D) Shikimic acid (binding affinity: -6 kcal/mol), (E) 4- Coumaric acid (binding affinity: -6.2 kcal/mol), (F) Caffeic acid (binding affinity: -6.4 kcal/mol) (G) 2,4- Quinolinediamine (binding affinity: -6.3 kcal/mol). Docking of the *Rhododendron* molecules against the target proteins was done using the PyRx software and analyses of the docking results were carried out by using the software Biovia Discovery studio client 2020.

Preprints (www.preprints.org) | NOT PEER-REVIEWED | Posted: 24 August 2020 doi:10.20944/preprints202008.0530.v1

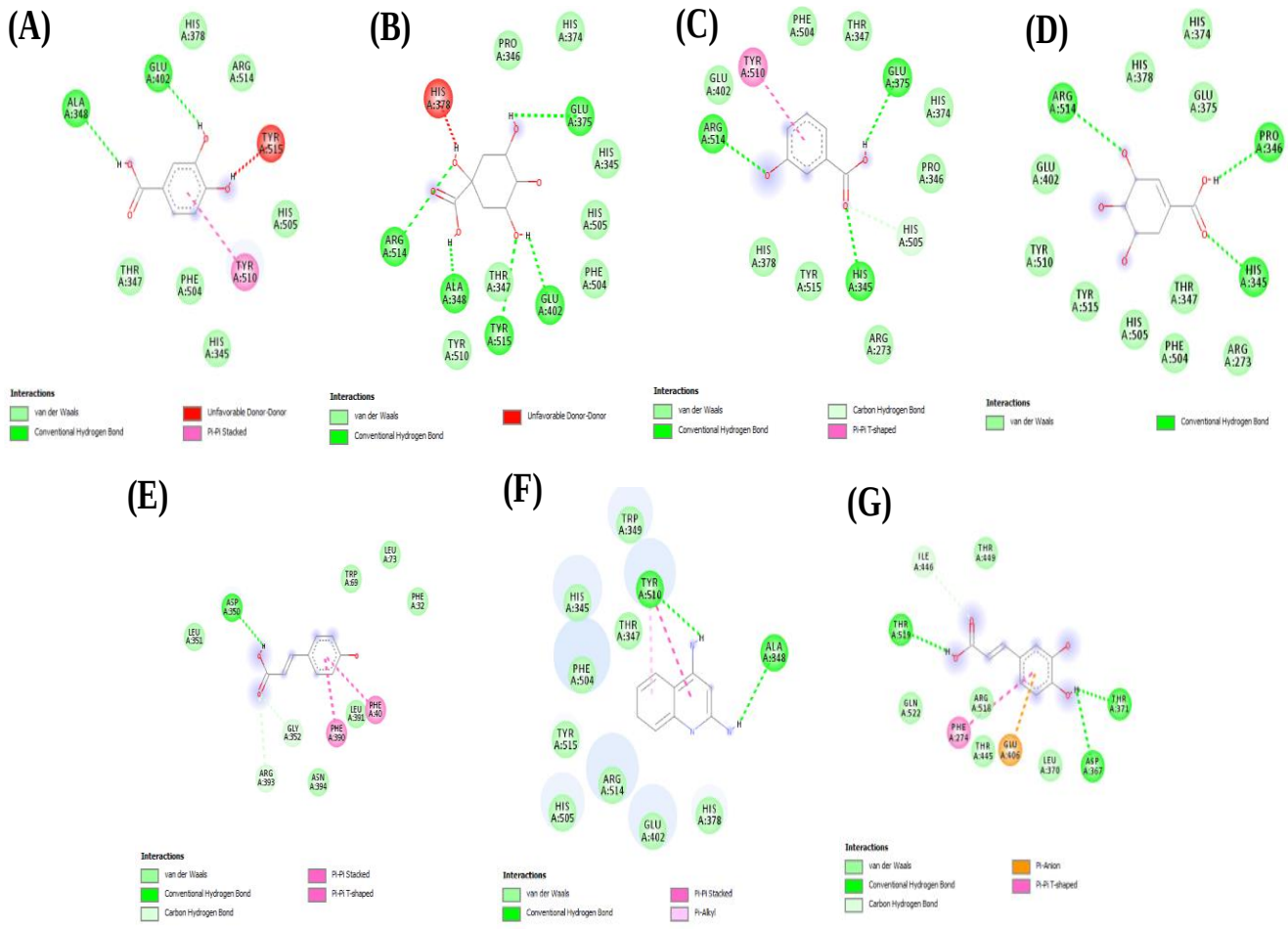

Fig. S6. Amino acid residue interactions of ACE2 host cell receptor (PDB ID-1R4L) binding with **(A)** Protocatechuic acid **(B)** Quinic acid **(C)** 3- Hydroxybenzoic acid **(D)** Shikimic acid **(E)** 4- Coumaric acid **(F)** Caffeic acid and (G) 2,4- Quinolinediamine.

Preprints (www.preprints.org) | NOT PEER-REVIEWED | Posted: 24 August 2020 doi:10.20944/preprints202008.0530.v1

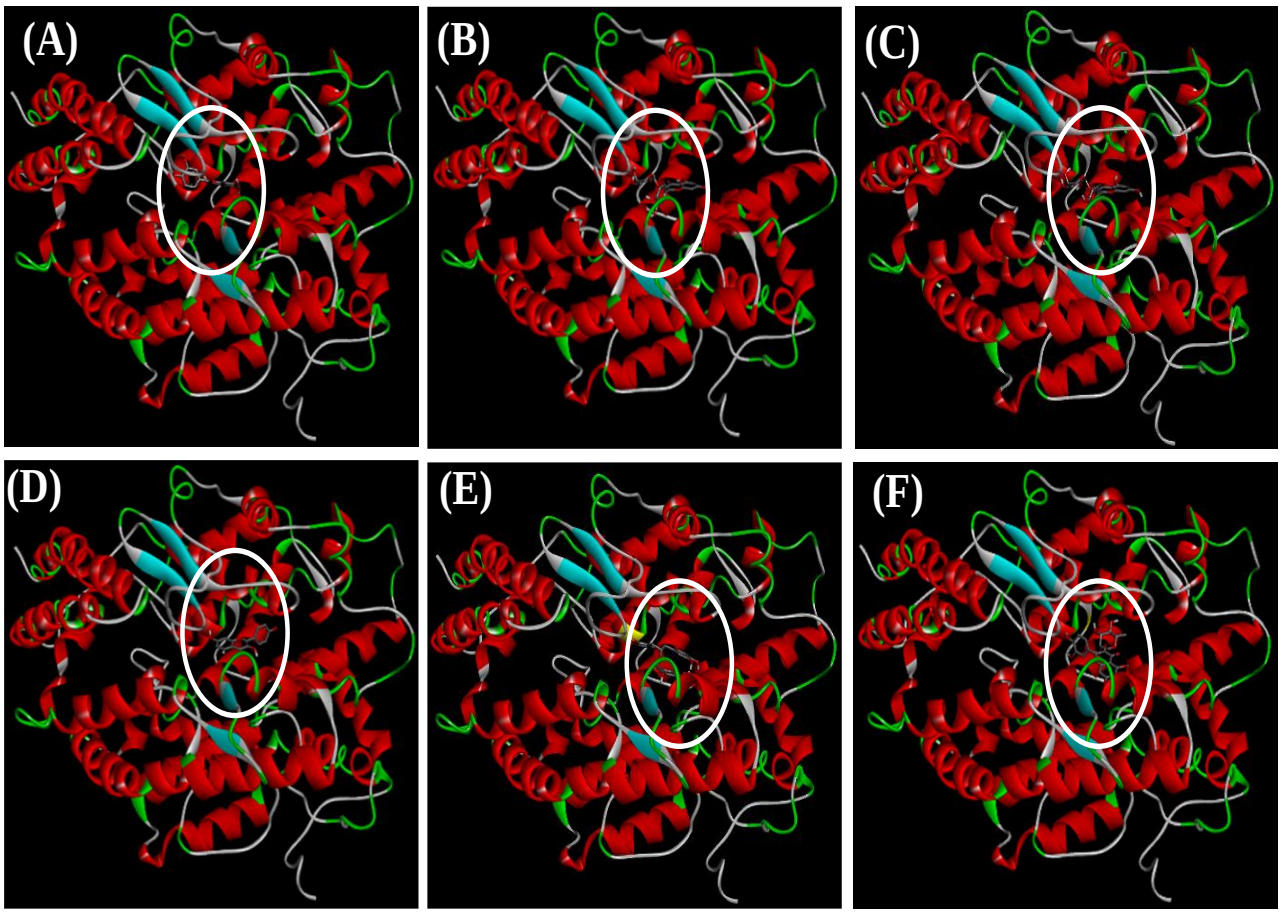

Fig. S7. Active site docking simulation of the interaction between ACE2 host cell receptor (PDB ID-1R4L) and **(A)** Quercetin (binding affinity: -8.9 kcal/mol), **(B)** Quercetin-O-pentoside (binding affinity: -9.9 kcal/mol), **(C)** Kaempferol-O-pentoside (binding affinity: -9.7 kcal/mol), **(D)** Kaempferol (binding affinity: -8.4 kcal/mol), **(E)** Epicatechin gallate (binding affinity: -10.1 kcal/mol), **(F)** Quercetin-O-rhamnoside (binding affinity: -10.2 kcal/mol). Docking of the *Rhododendron* molecules against the target proteins was done using the PyRx software and analyses of the docking results were carried out by using the software Biovia Discovery studio client 2020.

Preprints (www.preprints.org) | NOT PEER-REVIEWED | Posted: 24 August 2020 doi:10.20944/preprints202008.0530.v1

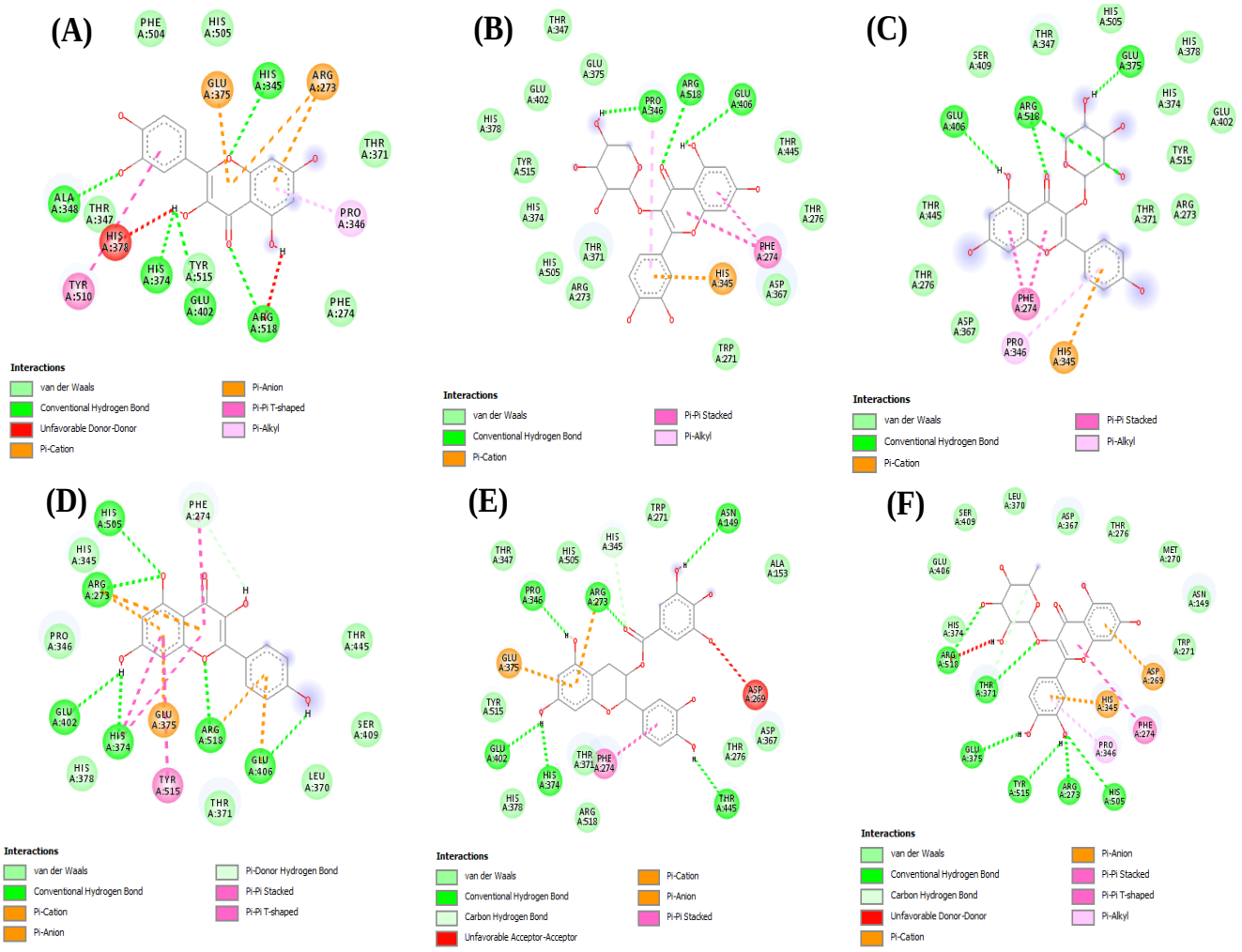

Fig. S8. Amino acid residue interactions of ACE2 host cell receptor (PDB ID-1R4L) binding with (A) Quercetin, (B) Quercetin-O-pentoside, (C) Kaempferol-O-pentoside, (D) Kaempferol, (E) Epicatechin gallate and (F) Quercetin -O- rhamnoside.